Discovery of the Plagiogranites in the Diyanmiao Ophiolite, Southeastern Central Asian Orogenic Belt, Inner Mongolia, China and Its Tectonic Significance

LI Yingjie[1,*], WANG Jinfang[1], WANG Genhou[2], DONG Peipei[1], LI Hongyang[1] and HU Xiaojia[3]

1 *School of Nature Resources, Hebei GEO University, Shijiazhuang 050031, China*
2 *School of the Earth Sciences and Resources, China University of Geosciences, Beijing 100083, China*
3 *Tianjin Institute of Geology and Mineral Resources, Tianjin 300170, China*

Abstract: In this study, plagiogranites in the Diyanmiao ophiolite of the southeastern Central Asian Orogenic Belt (Altaids) were investigated for the first time. The plagiogranites are composed predominantly of albite and quartz, and occur as irregular intrusive veins in pillow basalts. The plagiogranites have high SiO_2 (74.37–76.68wt%) and low Al_2O_3 (11.99–13.30wt%), and intensively high Na_2O (4.52–5.49wt%) and low K_2O (0.03–0.40wt%) resulting in high Na_2O/K_2O ratios (11.3–183). These rocks are classified as part of the low-K tholeiitic series. The plagiogranites have low total rare earth element contents (∑REE)(23.62–39.77ppm), small negative Eu anomalies (δEu=0.44–0.62), and flat to slightly LREE-depleted chondrite-normalized REE patterns ($(La/Yb)_N$=0.68–0.76), similar to N-MORB. The plagiogranites are also characterized by Th, U, Zr, and Hf enrichment, and Nb, P, and Ti depletion, have overall flat primitivemantle-normalized trace element patterns. Field and petrological observations and geochemical data suggest that the plagiogranites in the Diyanmiao ophiolite are similar to fractionation-type plagiogranites. Furthermore, the REE patterns of the plagiogranites are similar to those of the gabbros and pillow basalts in the ophiolite. In plots of SREE–SiO_2, La–SiO_2, and Yb–SiO_2, the plagiogranites, pillow basalts, and gabbros show trends typical of crystal fractionation. As such, the plagiogranites are oceanic in origin, formed by crystal fractionation from basaltic magmas derived from depleted mantle, and are part of the Diyanmiao ophiolite. LA–ICP–MS U–Pb dating of zircons from the plagiogranites yielded ages of 328.6±2.1 and 327.1±2.1Ma, indicating an early Carboniferous age for the Diyanmiao ophiolite. These results provide petrological and geochronological evidence for the identification of the Erenhot–Hegenshan oceanic basin and Hegenshan suture of the Paleo-Asian Ocean.

Key words: Plagiogranite, LA–ICP–MS U–Pb zircon dating, Early-Carboniferous, Diyanmiao ophiolite, southeastern Altaids

1 Introduction

Oceanic plagiogranites are considered to be the product of fractional crystallization of basaltic melts, and are the most important silicic rocks in ophiolites. These rocks represent the final stage of oceanic crustal evolution (Coleman and Peterman, 1975). Oceanic plagiogranites are also an important rock type for the accurate dating of zircons in ophiolites (Grimes et al., 2008, 2013; Furnes and Dilek, 2017). Detailed research on the formation and evolution of plagiogranites has shown that different types of plagiogranites may form during different stages of the evolution of ophiolites, from mid-ocean ridge spreading through to the migration, subduction, and obduction stages (Searle and Malpas, 1980; Gerlach et al., 1981; Pedersen and Malpas, 1984; Pearce, 1989; Flagler and Spray, 1991; Bebout and Barton, 1993; Wang Xiang, 1993; Peters and Kamber, 1994; Jafri et al., 1995; Amri et al., 1996; Bébien et al., 1997; Whitehead et al., 2000; Scarrow et al., 2001; Li Wuxian and Li Xianhua, 2003; Li and Li, 2003; Jian et al., 2003a, b; Zhang Qi et al., 2008; France et al., 2010; Dilek and Furnes, 2014; Santosh et al., 2016). Four genetic types of plagiogranites have been recognized: fractionation-, shearing-, subduction-, and obduction-type (Coleman and Peterman, 1975; David et al., 1981;

* Corresponding author. E-mail: yingjieli820@163.com

Pedersen and Malpas, 1984; Sorensen and Grossman, 1989; Pearce, 1989; Flagler and Spray, 1991; Claoue-long et al., 1995; Amri et al., 1996; Floyd et al., 1998; Cox et al., 1999; Li Wuxian and Li Xianhua, 2003; Li and Li, 2003; Koepke et al., 2004, 2007; Yoshikawa and Ozawa, 2007; Skjerlie et al., 2000; Whitehead et al., 2000; Freund et al., 2014; Gai Yongsheng et al., 2015; Jiang et al., 2015; Kang Lei et al., 2015; Zeng et al., 2015; Yang et al., 2017). Therefore, it is important to identify different kinds of plagiogranites formed in the different evolutionary stages of ophiolites through field and laboratory investigations, as well as accurately dating such rocks, as this enables the reconstruction of the regional tectonic evolution of orogenic belts.

The Central Asian Orogenic Belt (also known as the Altaids) is a vast accretionary orogen between the Siberian Craton (SC) to the north and Tarim and North China cratons (NCC) to the south. The belt is considered to be the world's largest Phanerozoic accretionary orogen (Fig. la; Şengör *et al*., 1993; Badarch et al., 2002; Jahn et al., 2004; Windley et al., 2001, 2007; Xiao et al., 2009 , 2015; Xiao and Santosh, 2014; Kröner et al., 2017; Safonova, 2017).The southeastern Altaids, spreading through the Inner Mongolia and Xinjiang regions in North China, is a key area for understanding the Paleozoic tectonic evolution of the Altaids, and is characterized by a series of island arcs, fore-arc or back-arc basins, ophiolitic belts and microcontinents from the Neoproterozoic to Mesozoic (Wang and Liu, 1986; Shao, 1989; Tang, 1990; Şengör and Natal'in, 1996; Badarch et al., 2002; Khain et al., 2003; Kovalenko et al., 2004; Xiao et al., 2003, 2009, 2010, 2013; Li, 2006; Windley et al., 2007; Kröner et al., 2008, 2011; Xu et al., 2013; Zhao et al., 2013). The tectonic evolution of the southeastern Altaids has long been a subject of research (Tang and Yan,1993; Xiao et al., 2003, 2009; Miao et al., 2008; Jian et al., 2008, 2010; Zhang et al., 2011; Zhao et al., 2013; Kang Jianli et al., 2016; Wang Dandan et al., 2016; Zhu Junbin and Ren Jishun, 2017; Zhang Yongsheng et al., 2017; Dang Zhicai et al., 2018), but the precise timing of the formation of the Paleo-Asian Ocean and the exact location and timing of its closure remain controversial (Şengör and Natal'in, 1996; Miao et al., 2008; Xu et al., 2013; Zhao et al., 2016).

From south to north, five ENE–WSW-trending tectonic zones can be identified in the southeastern Altaids of Inner Mongolia, which are the southern early to mid-Paleozoic orogenic belt (SOB), the Hunshandake block (HB) (Solonker suture zone), the northern early to mid-Paleozoic orogenic belt (NOB), the Erenhot–Hegenshan ophiolite accretionary belt (EHOB), and the Uliastai continental margin (Xiao et al., 2003; Jian et al., 2012) (Fig. 1b).

The recently discovered Diyanmiao ophiolite is in the eastern part of the EHOB (Fig. 1b). The NE-trending EHOB extends ca. 500 km from Erenhot in the southwest to the Hegenshan Mountains in the northeast, and from west to east contains numerous ophiolite slices, including the Erenhot, Hegenshan, Meilaotewula, and Diyanmiao ophiolites (Li et al., 2015). To date, the EHOB has been extensively studied, but there are many conflicting ages for ophiolites in this region (Miao et al., 2008; Jian et al., 2012). For example, fossils in cherts in fault contact with the Hegenshan ophiolite suggest a Middle–Late Devonian age (Liu, 1983; Liang, 1991). Proposed ages from isotopic dating encompass the Late Devonian to early Carboniferous (e.g. Huang Bo et al., 2016), late Silurian to early Carboniferous (e.g. Liu Jiayi, 1983; Liang Rixuan, 1994), Early Devonian (e.g. Bao Zhiwei et al., 1994), early Carboniferous (e.g. Zhang et al., 2015; Cheng Yinhang et al., 2016; Wang Shuqing et al., 2017; Zhu Junbin and He Zhengjun, 2017; Li Yingjie et al., 2015, 2018), late Carboniferous to early Permian (Miao et al., 2008; Wang Jinfang et al., 2017a, b), Late Cretaceous (Nozaka and Liu, 2002), and two periods in the early Carboniferous and Early Cretaceous (Jian et al., 2012). The reasons for these conflicting ages can be attributed to two aspects. Firstly, it is not clear if the fossil-bearing sedimentary rocks overlie the ophiolite rocks. Secondly, it is difficult to obtain magmatic zircons ideal for isotopic dating from the mafic rocks of the ophiolites. However, plagiogranites represent ideal material for the dating of magmatic zircons in ophiolites and can provide reliable formation ages (e.g. Pidgeon et al., 1998; Buchan et al., 2005; Baines et al., 2005; Li et al., 2013; Yin Zhengxin et al., 2015).

Therefore, further detailed studies of typical ophiolites in the southeastern Altaids are required. The Diyanmiao ophiolite preserves a relatively complete suite of lithological units (Li Yingjie et al., 2012; 2013; 2018; Li et al., 2018), and is an ideal unit in which to carry out an ophiolite study. Zircon U–Pb dating of gabbros in the Diyanmiao ophiolite indicates its formation in the early Carboniferous (Li et al., 2018). However, the Diyanmiao ophiolite has not been extensively studied. Plagiogranites have been recently identified in the Diyanmiao ophiolite. In this study, we carried out a detailed geological and petrological investigation, and acquired new LA–ICP–MS zircon U–Pb age and major–trace element data for the plagiogranites. The objectives of this study were to: (1) determine the age of the plagiogranites and constrain the age of the EHOB; (2) constrain the origin of the plagiogranites based on detailed geochemical analysis; and (3) to constrain the late Paleozoic tectonic evolution of the

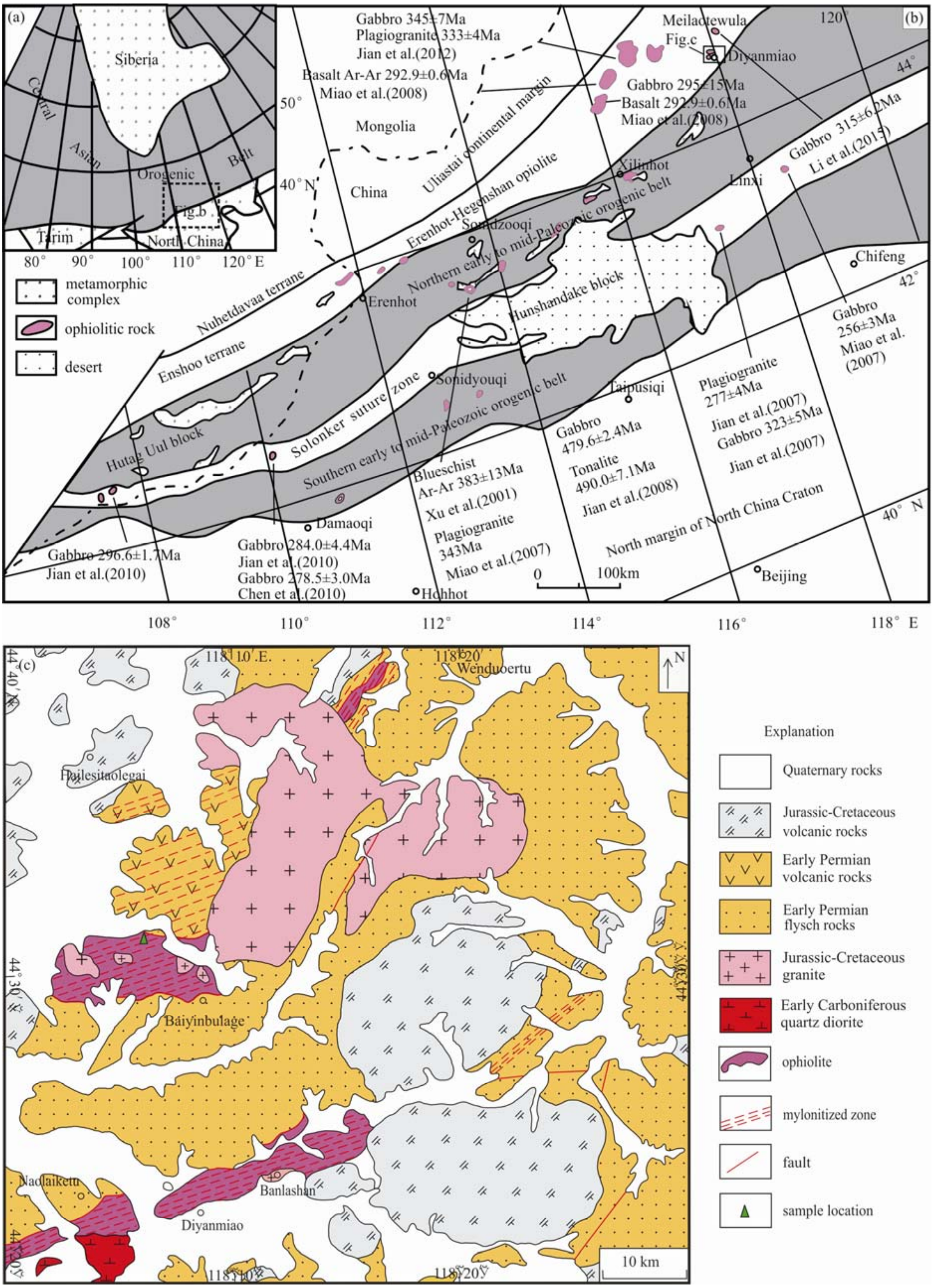

Fig. 1. (a), Tectonic framework of the north China-Mongolia segment of the Central Asian Orogenic Belt (modified from Jahn, 2004); (b), sketch geological map of the northern China-Mongolia tract (modified from Badarch et al., 2002; Miao et al., 2008; Xiao et al., 2009; Jian et al., 2010, 2012; Zhang et al., 2015b). Some of the Paleozoic isotopic ages of ophiolitic mélanges are shown (modified from Jian et al., 2008, 2010, 2012; Xiao et al., 2009; li et al., 2013a; li et al., 2015); (c), simplified geological map of the Diyanmiao area (modified from li et al., 2012), showing the sample location of this study.

EHOB.

2 Geology and Petrography

The Diyanmiao ophiolite is located in central Inner Mongolia, China (118°00′–118°30′ E, 44°20′–44°40′N; Fig. lb and c). The ophiolite can be divided into the northern Baiyinbulage subzone and southern Naolaiketu ophiolite subzone (Fig. 1c). Each subzone strikes ENE–WSW to NE–SW with a length of ca. 100 km and width of 6 km (Fig. 1c). The Diyanmiao ophiolite is well exposed and consists mainly of harzburgite, layered gabbro, medium- to coarse-grained isotropic gabbro, fine-grained isotropic gabbro, anorthosite, spilite, pillow basalt, variolite, brecciated basalt, keratophyre, baschtauite, and overlying chert. The ophiolite represents a well-preserved original ophiolitic sequence, which from base to top includes harzburgite, layered gabbro, medium- to coarse-grained isotropic gabbro, fine-grained isotropic gabbro, anorthosite, spilite, pillow basalt, and chert. Most of these rocks are continuously exposed in an antiform (Li Yingjie et al., 2012, 2013; Li et al., 2018). Ductile shear zones are developed in the Diyanmiao ophiolite. Locally, the ophiolite is strongly deformed, and mylonitized and foliated rocks and tectonic schists are present. The Diyanmiao ophiolite is a structural lens that was emplaced into the early Permian strata of the Shoushangou formation and Dashizhai formation. Rocks of the Shoushangou formation and Dashizhai formation near the ophiolite belt exhibit extensive cleavage development, fragmentation, hyllitization, and mylonitization (Li et al., 2018).

Plagiogranites are exposed both in the northern Baiyinbulage subzone and southern Naolaiketu ophiolite subzone. In the former, five irregular short veins of plagiogranites (named N_I to N_V) intrude into pillow basalts (Fig. 2a). These plagiogranite veins have lengths of up to several meters and widths of 0.5–1.0m (Fig. 2a). No obvious deformation was observed in the plagiogranites (Fig. 2c). The wall rocks of the plagiogranites are pillow basalts, with a typical pillow structure (Fig. 2b). In the

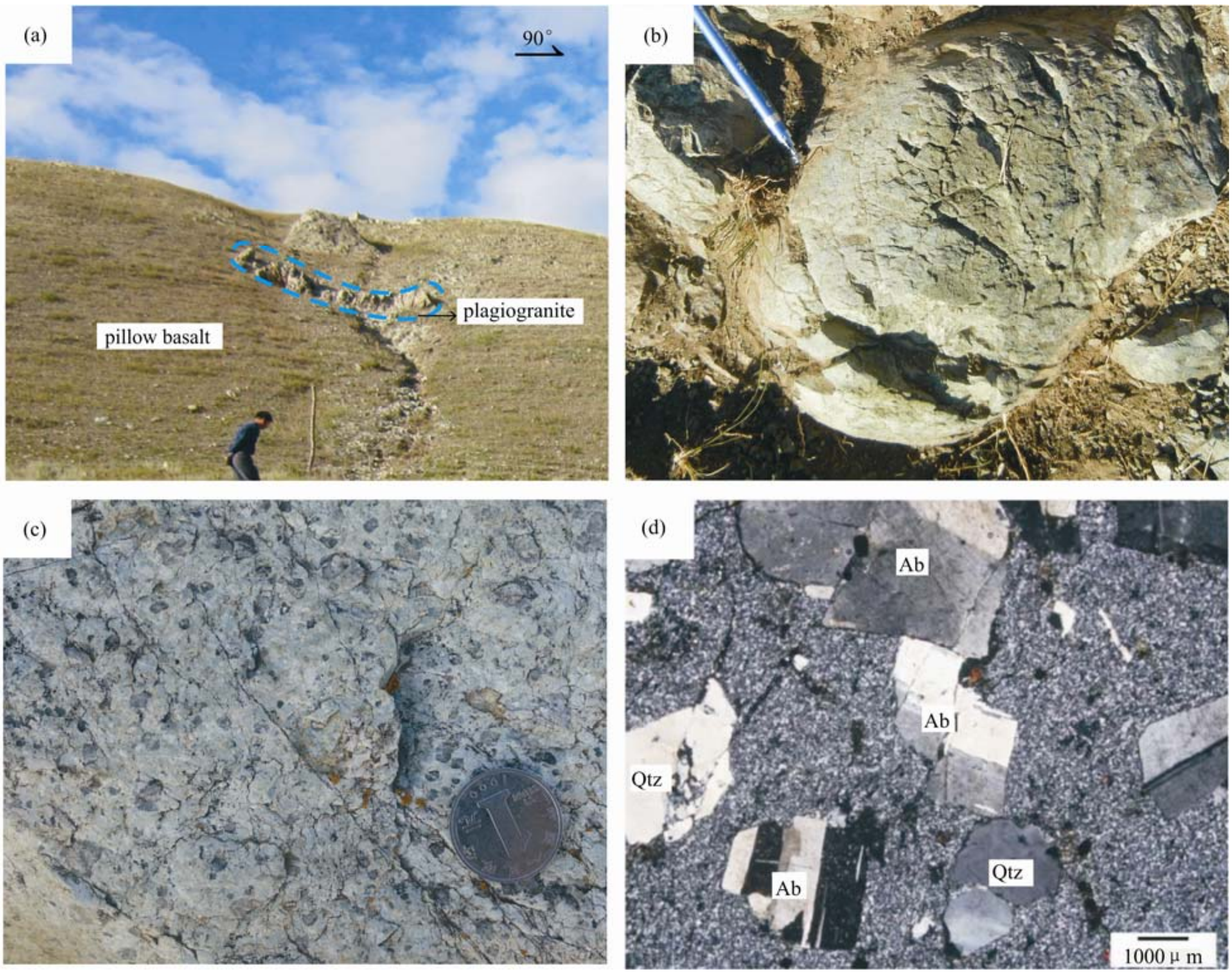

Fig. 2. Field occurrence and microtextures of plagiogranites and pillow basalts in the Diyanmiao ophiolite.
(a), contact relationship between plagiogranites and pillow basalts; (b), field feature of pillow basalts; (c), field feature of plagiogranites; (d), microtextures of plagiogranites. Pl-plagioclase; Ab, Albite; Qtz, quartz.

southern Naolaiketu ophiolite subzone, two irregular and short veins of plagiogranite (S_I and S_{II}) intrude into gabbros. These veins have lengths of a few meters and widths of 0.5–1.0m.

These rocks have a porphyritic texture (Fig. 2c and d) and the phenocrysts include altered plagioclase and quartz. Most mineral grains are 0.05 to 0.6mm in size. Plagioclase is hypidiomorphic tabular, exhibits partial albite twinning, is mainly albitic, and has been partly altered to kaolin and sericite. Quartz within these samples is allotriomorphic granular and occurs within interstices between plagioclase grains. The groundmass is mainly microcrystalline plagioclase and quartz.

The plagiogranite samples used for this study were collected from plagiogranite veins N_I and N_{II} in the northern Baiyinbulage ophiolite subzone (Fig. 2a). The sample locations (118°05′24″ E, 44°30′59″N) are shown in Fig. 1c.

3 Analytical Methods

3.1 Zircon U-Pb dating analyses

Zircon grains were separated by conventional magnetic and density techniques, and then selected by hand-picking under a binocular microscope. Representative zircon grains along with TEMORA standard (417Ma) were embedded in epoxy resin and polished to expose the crystals for dating. Transmitted and reflected light micrographs as well as cathodoluminescence (CL) images were obtained for the polished zircon grains before U–Pb isotope analyses in order to reveal their internal structure and external morphology and guide the selection of potential analytical spots.

The CL images were made using a JSM6510 Scanning electron microscope with GATAN CL at Beijing Gaonianlinghang Geo Analysis Co. Ltd., Beijing.

Zircon grains from the plagiogranites were dated in situ on an ArF-excimer (193-nm wavelength) laser ablation multiple-collector inductively coupled plasma mass spectrometer (LA-ICP-MS) at the Tianjin Institute of Geology and Mineral Resources, China Geological Survey. The ICP-MS used was Neptune made by Thermo Fisher, and the UP193-FX ArF laser ablation system (ESI Company) was used for the laser ablation experiments. The instrumental conditions and analytical processes were similar to those described by Hou et al. (2009). U and Pb

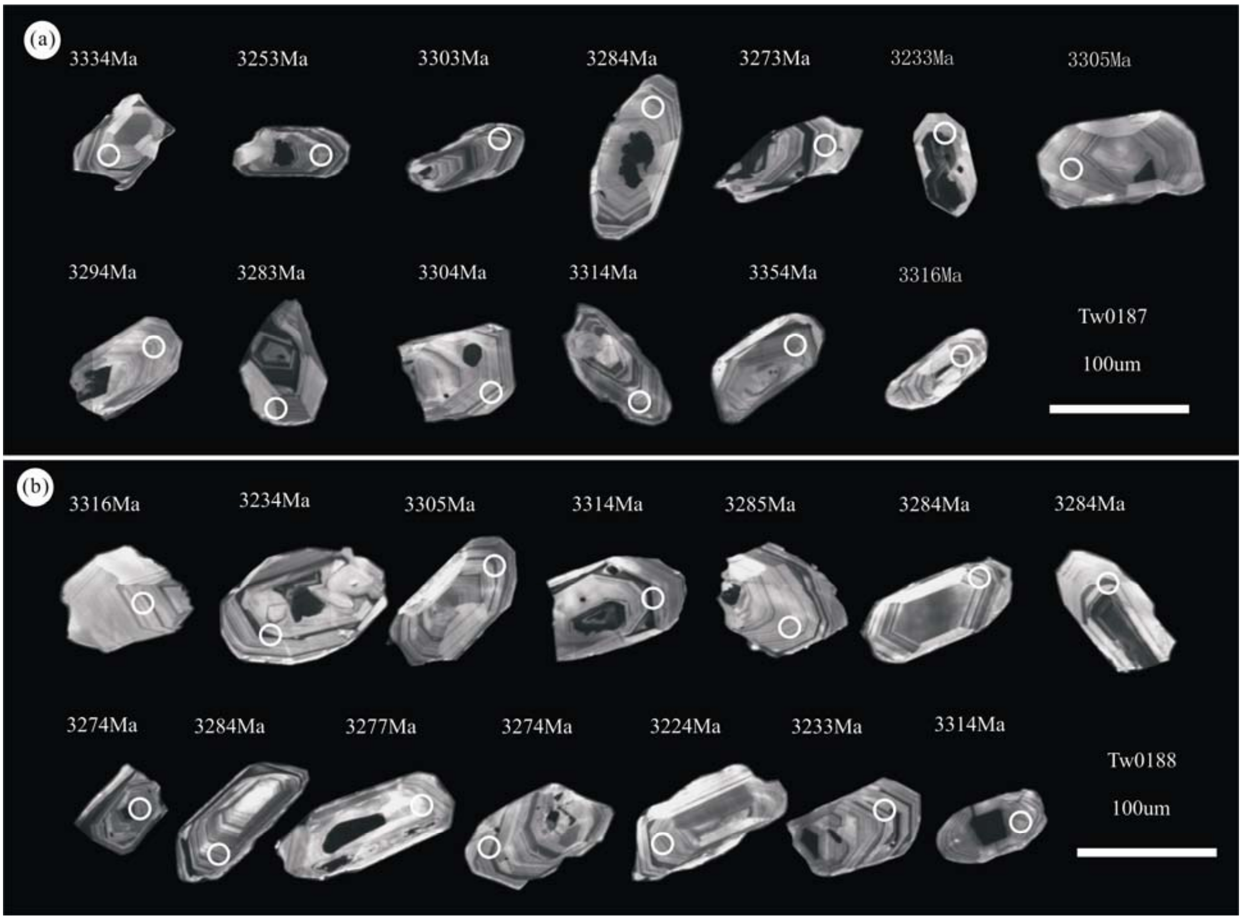

Fig. 3. CL cathodoluminescence images of representative zircon grains and their apparent ages of samples of plagiogranites from the Diyanmiao ophiolite: (a) Tw0187; (b) Tw0188.

concentrations were calibrated by using TEMORA and GJ -1 as external standards (Jackson et al., 2004). $^{207}Pb/^{206}Pb$, $^{206}Pb/^{238}U$, $^{207}Pb/^{235}U$, and $^{208}Pb/^{232}Th$ ratios, calculated using the ICPMSDataCal program (Liu et al., 2009) and the Isoplot program (Ludwig, 2003), were corrected for both instrumental mass bias and elemental and isotopic fractionation by using standard glass NIST612 as an external standard. The age data are in Table 1.

3.2 Mineral geochemistry

Electron microprobe analysis was carried out on plagioclase with a JEOL JXA 8100 M electron microprobe (EMPA) at the Hebei Geology and Mineral Institute, China. The operating conditions were as follows: accelerating voltage 15kV, beam current 20nA, beam diameter 1μm. Peak and background counting times were set at 30s. All data were corrected with standard ZAF correction procedures (Table 2). Natural minerals and synthetic glasses were used as standards. Detailed procedure has been described in Wang et al. (2009).

3.3 Major and trace elemental analyses

Major elements were analyzed by X-ray fluorescence (XRF) (Rigaku 3270E) at the Tianjin Institute of Geology and Mineral Resources, China Geological Survey. Analytical precision was generally better than 2% for most oxides, monitored by analyses of Chinese national standard samples GSR–1, GSR–2 and GSR–3. Trace element data also were obtained at the Tianjin Institute of Geology and Mineral Resources, China Geological Survey by inductively coupled plasma mass spectrometer (ICP-MS) using the analytical procedure of Liu et al. (2008). The analytical precisions for most trace elements are greater than 5%, monitored by analyses of Chinese national standard samples GSR–1 and GSR–3. The analytical precision was better than 5% for trace elements. The major and trace elemental data from plagiogranite samples are listed in Table 3.

Table 2 Electron microprobe analyses of plagioclases in the plagiogranite from the Diyanmiao ophiolite

Sample	b0124	b0124	b0124	b0183
Rock type	plagiogranite	plagiogranite	plagiogranite	plagiogranite
Mineral	Pl	Pl	Pl	Pl
SiO_2	68.72	68.93	68.73	68.56
Al_2O_3	19.92	19.72	18.93	20.15
FeO	0.08	0.01	1.35	-
MgO	-	-	0.14	-
CaO	0.36	0.37	0.14	0.66
Na_2O	11.76	12.05	10.96	11.52
K_2O	0.19	0.12	1.08	0.03
Total	101.07	101.19	101.33	100.93
Cations per 32 oxygens				
Si	2.979	2.983	3.015	2.970
Al	1.018	1.006	0.979	1.029
Ca	0.017	0.017	0.007	0.031
Na	0.988	1.011	0.932	0.968
K	0.011	0.006	0.060	0.002
Sum	5.012	5.023	4.993	4.100
An	1.65	1.65	0.67	3.07
Ab	97.30	97.73	93.31	96.76
Or	1.05	0.61	6.02	0.17

Table 1 LA-ICP-MS zircon U-Pb isotopic analysis of plagiogranites in the Diyanmiao ophiolite

Spots no.	Element (ppm)		Th/U	Isotopic ratios						Apparent age (Ma)					
	Th	U		$^{206}Pb/^{238}U$	1σ	$^{207}Pb/^{235}U$	1σ	$^{207}Pb/^{206}Pb$	1σ	$^{206}Pb/^{238}U$	1σ	$^{207}Pb/^{235}U$	1σ	$^{207}Pb/^{206}Pb$	1σ
TW0187 plagiogranite															
TW0187-01	23	88	0.26	0.0531	0.0007	0.3950	0.0412	0.0540	0.0056	333	4	338	35	371	234
TW0187-02	45	115	0.39	0.0516	0.0005	0.3829	0.0236	0.0538	0.0033	325	3	329	20	362	139
TW0187-03	62	160	0.39	0.0525	0.0006	0.4015	0.0219	0.0555	0.0030	330	3	343	19	433	119
TW0187-04	23	73	0.31	0.0522	0.0006	0.3824	0.0405	0.0531	0.0056	328	4	329	35	335	240
TW0187-05	133	219	0.61	0.0520	0.0005	0.3880	0.0140	0.0541	0.0019	327	3	333	12	377	79
TW0187-06	189	325	0.58	0.0514	0.0006	0.3781	0.0221	0.0534	0.0031	323	3	326	19	346	132
TW0187-07	15	40	0.37	0.0526	0.0009	0.3917	0.0743	0.0540	0.0112	331	6	336	64	371	466
TW0187-08	15	56	0.27	0.0523	0.0007	0.3871	0.0523	0.0537	0.0073	329	4	332	45	358	306
TW0187-09	148	289	0.51	0.0522	0.0005	0.3807	0.0247	0.0529	0.0034	328	3	328	21	324	145
TW0187-10	20	68	0.29	0.0525	0.0006	0.3927	0.0484	0.0542	0.0067	330	4	336	41	381	278
TW0187-11	11	50	0.23	0.0526	0.0007	0.3856	0.0630	0.0532	0.0091	330	5	331	54	336	389
TW0187-12	26	88	0.30	0.0527	0.0006	0.4001	0.0338	0.0551	0.0048	331	4	342	29	416	196
TW0187-13	16	53	0.30	0.0533	0.0007	0.4007	0.0690	0.0545	0.0097	335	4	342	59	392	400
TW0188 plagiogranite															
TW0188-01	8	38	0.20	0.0527	0.0009	0.4014	0.0840	0.0553	0.0126	331	6	343	72	424	509
TW0188-02	113	165	0.68	0.0525	0.0006	0.4077	0.0300	0.0563	0.0041	330	4	347	26	464	161
TW0188-03	15	59	0.25	0.0526	0.0008	0.3884	0.0741	0.0536	0.0103	330	5	333	64	353	435
TW0188-04	100	172	0.58	0.0527	0.0006	0.3897	0.0322	0.0537	0.0044	331	4	334	28	357	185
TW0188-05	14	50	0.27	0.0521	0.0008	0.3893	0.0617	0.0541	0.0085	328	5	334	53	377	354
TW0188-06	44	95	0.46	0.0521	0.0006	0.3901	0.0293	0.0543	0.0041	327	4	334	25	384	169
TW0188-07	20	73	0.28	0.0522	0.0006	0.3933	0.0403	0.0547	0.0057	328	4	337	34	399	232
TW0188-08	35	117	0.30	0.0522	0.0007	0.3866	0.0317	0.0537	0.0043	328	4	332	27	360	182
TW0188-09	36	123	0.29	0.0522	0.0006	0.3885	0.0224	0.0539	0.0031	328	4	333	19	368	130
TW0188-10	14	50	0.28	0.0520	0.0011	0.3804	0.1080	0.0531	0.0154	327	7	327	93	332	658
TW0188-11	23	82	0.28	0.0521	0.0007	0.3838	0.0408	0.0534	0.0056	327	4	330	35	346	237
TW0188-12	29	91	0.31	0.0512	0.0006	0.3791	0.0334	0.0537	0.0046	322	4	326	29	357	195
TW0188-13	77	153	0.50	0.0513	0.0006	0.3740	0.0213	0.0528	0.0029	323	3	323	18	322	124
TW0188-14	26	76	0.34	0.0513	0.0006	0.3777	0.0466	0.0534	0.0065	323	4	325	40	345	276

4 Analytical Results

4.1 LA-ICP-MS zircon U-Pb dating

U-Pb dating results for zircons from two plagiogranite samples (TW0187, TW0187) were listed in Table 1. The zircon grains from two plagiogranite samples range from 80 to 110m with length to width ratios of 2:1 to 3:1. Most grains are colorless to light yellow, transparent and euhedral with well-developed patchy oscillatory zoning in CL images (Fig. 3a, Fig. 3b), suggesting an acidic magmatic crystallization in ancient and modern oceanic plagiogranites (Belousova et al., 2002; Schwartz et al., 2005; Baines et al., 2009; Grimes et al., 2009). They have relatively low Th content (mostly 15–189ppm) and high U content (mostly 40–325ppm; Table 1), and the Th/U ratio varies from 0.23 to 0.61 (Table 1) indicating a magmatic origin of the zircon grains (Wu Yuanbao and Zheng Yongfei., 2004). 27 analyses on these zircons show good concordance on the $^{206}Pb/^{238}U$–$^{207}Pb/^{235}U$ concordia diagram and yield weighted mean $^{206}Pb/^{238}U$ ages of 328.6 ±2.1Ma and 327.1 ±2.1Ma (Fig. 4). The mean age is interpreted to be the crystallization age of the plagiogranites.

4.2 Mineral geochemistry

Electron microprobe analyses of plagioclase in the Diyanmiao plagiogranites were presented in Table 2. Plagioclases in the plagiogranites have high contents of albite (Ab) (93.31–97.73wt%), minor anorthite (An) (0.67 –3.07wt%) and orthoclase (Or) (0.61–6.02wt%).

4.3 Whole-rock geochemistry

The SiO_2 contents of four plagiogranite samples range from 74.37 to 76.68wt% (average=75.25wt%). The other major elements have the following concentrations: TiO_2=0.22–0.24wt % (average=0.23wt %); CaO=1.72–3.38wt% (average=2.26wt%); and MgO=0.52–1.53wt% (average=0.9wt%). $Mg^{\#}$ values vary from 32.45 to 55.66 (average=43.11) (Table 3). The plagiogranite samples are characterized by low Al_2O_3 (11.99–13.30wt%) and P_2O_5 (0.03–0.04wt %), and intensively high Na_2O (4.52–5.06wt%) and low K_2O (0.03–0.4wt%) resulting in Na_2O/

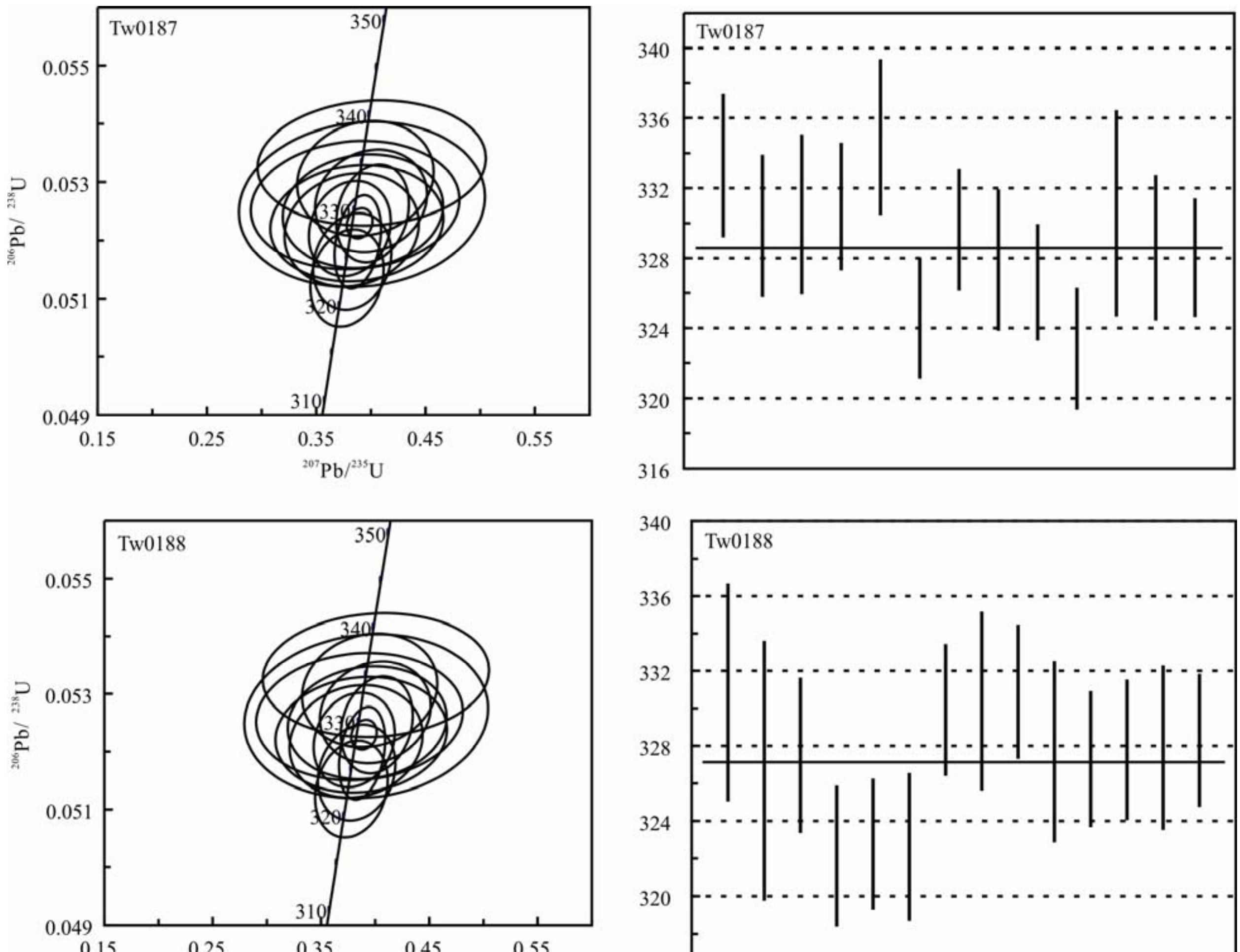

Fig. 4. Zircon U–Pb concordia diagrams and histograms of weighted mean ages of plagiogranites from the Diyanmiao ophiolite.

K_2O=11.3–183 and moderate A/CNK ratios (0.87–1.21). The rocks are aluminous–peraluminous. On a total alkalis–silica classification diagram (Fig. 5a), data for the plagiogranite samples plot in the granite field of the subalkaline series. On a SiO_2 vs. K_2O diagram (Fig. 5b), data for samples of plagiogranites and pillow basalts plot in the low-K tholeiite series, indicating a genetic relationship between the two rock types.

The plagiogranites have low ∑REE (23.62–39.77ppm), small negative Eu anomalies (δEu=0.44–0.62), and flat chondrite-normalized REE patterns ($(La/Yb)_N$=0.68–0.76) (Fig. 6a), similar to normal and transitional mid-ocean ridge basalts (N-MORB and T-MORB). In addition, the chondrite-normalized REE patterns of the plagiogranites are similar in shape, but show higher concentrations as compared with those of the pillow basalts and gabbros in the Diyanmiao ophiolite (Fig. 6a).

Primitive-mantle-normalized trace element patterns are characterized by Th, U, Zr, and Hf enrichment, and Nb, P, and Ti depletion. The plagiogranites have low Sr (78.2–146ppm) and high Yb and Y contents (1.96–3.56 and 14.8–27.9ppm, respectively), similar to other plagiogranites in ophiolites (Pearce et al., 1984; Zhang et al., 2008). Moreover, the plagiogranite trace element patterns are broadly similar to those for associated pillow basalts in the Diyanmiao ophiolite, but the plagiogranites have higher Th, U, Zr, Hf, Nb, and Ta contents and lower Ti contents (Fig. 6b). As such, the plagiogranites and gabbros in the Diyanmiao ophiolite have complementary trace element patterns (Fig. 6b).

All these features of the Diyanmiao plagiogranites are typical of fractionation-type plagiogranites, being similar to plagiogranites from the Troodos Ophiolite in Cyprus (Freund et al., 2014) and and the Jebel Fayyad plagiogranites from the Oman Ophiolite (Rollinson, 2009).

5 Discussion

5.1 Origin of the plagiogranites

Previous research has indicated that silicic rocks in ophiolites form in different stages, from mid-ocean ridge spreading through to the migration, subduction, and obduction stages. The different genetic types of plagiogranites are as follows (Li and Li, 2003). (1) Fractionation-type plagiogranites (i.e., oceanic plagiogranites) form by fractional crystallization and differentiation of oceanic basaltic magmas at low pressures, which typically form small dikes. Field observations indicate that fractionation-type plagiogranites are typically located in the upper gabbroic and basaltic rocks of an ophiolite sequence. The crystallization age of this type of plagiogranite represents a minimum age for the oceanic crust (Coleman and Peterman, 1975; David et al., 1981; Amri et al., 1996; Floyd et al., 1998; Claoue-long et al., 1995; Li Xianwu and Li Xianhua, 2003; Freund et al., 2014). (2) Shearing-type plagiogranites form by the partial melting of ophiolitic gabbros (or basalts) within shear zones, which develop in the lower part of the oceanic crust due to plate movement. This type of plagiogranite is generally produced in or near a ductile shear zone in gabbro from the lower ophiolite sequence, and forms a fine-grained vein network (length<1m). These plagiogranites are slightly younger than the age of the associated section of oceanic crust (Pedersen and Malpas, 1984; Flagler and Spray, 1991; Koepke et al., 2004, 2007; Grimes et al., 2013). (3) Subduction-type plagiogranites are formed by the partial melting of oceanic crust and overlying abyssal deposits during subduction. These plagiogranites are commonly found in the mantle

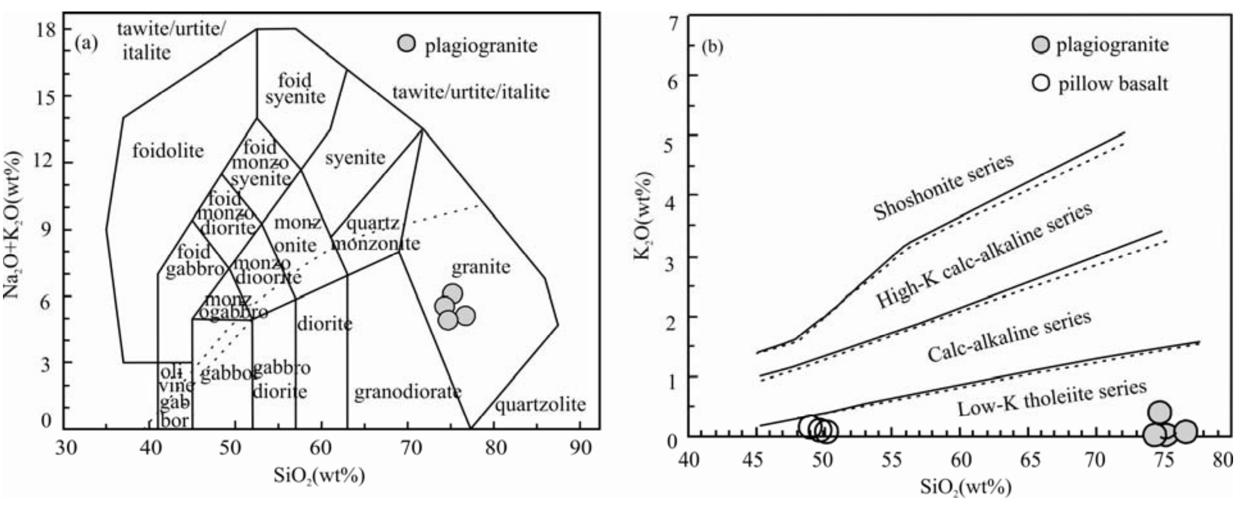

Fig. 5. TAS classification diagram (after Le Maitre, 2002) of the plagiogranite in Diyanmiao ophiolite (a) and K_2O vs. SiO_2 diagrams of the plagiogranite and pillow basalt in the Diyanmiao ophiolite (b).

Table 3 major (wt%), trace element (ppm) analyzing results of the plagiogranites, pillow basalts and gabbros in the Diyanmiao ophiolite

Rock type	plagiogranite	plagiogranite	plagiogranite	plagiogranite	pillow basalt	pillow basalt	pillow basalt	gabbro	gabbro	gabbro	gabbro
Sample	41730	41731	41732	41733	GS4590-1	GS4590-2	XGS01-1	XT1214-2	XT1214-3	GS3432-1	GS3432
SiO_2	75.25	74.37	76.68	74.71	50.17	48.96	49.68	45.49	45.94	45.53	46.84
Al_2O_3	12.91	13.23	11.99	13.30	14.12	14.61	15.81	17.05	15.19	16.35	15.25
Fe_2O_3T	2.05	2.11	1.99	2.27	8.34	9.00	8.82	4.82	7.26	5.11	4.98
CaO	1.84	3.38	2.11	1.72	9.94	8.35	5.26	17.32	16.94	19.54	19.47
MgO	0.74	0.52	0.79	1.53	10.3	11.3	11.61	10.64	9.86	8.58	8.71
K_2O	0.04	0.03	0.07	0.40	0.08	0.15	0.11	0.03	0.02	0.01	0.02
Na_2O	5.06	5.49	5.11	4.52	2.51	3	3.80	0.51	0.42	0.3	0.3
TiO_2	0.22	0.24	0.22	0.22	0.55	0.62	0.64	0.14	0.31	0.19	0.14
P_2O_5	0.04	0.03	0.03	0.04	0.03	0.03	0.03	0.03	0.08	0.03	0.04
MnO	0.02	0.03	0.03	0.03	0.16	0.17	0.14	0.14	0.15	0.13	0.14
LOI	1.79	0.54	0.90	1.13	4.05	4.24	4.03	3.44	3.12	3.81	3.65
TOTAL	99.80	100.00	99.92	99.77	99.87	99.98	99.48	96.22	96.24	95.82	95.93
Na_2O/K_2O	151.5	183	73	11.3	2.59	20	34.55	17	21	30	15
$Mg^{\#}$	41.16	32.45	43.16	55.66	70.89	71.18	72.13	80.03	71.02	75.26	75.87
Rb	1.21	0.97	1.47	4.41	0.8	1.4	1.89	0.61	0.42	0.20	0.61
Cr	5.75	5.07	6.52	4.44	520.9	712.5	574	8.85	11.9	9.19	8.85
Co	3.51	2.51	2.90	4.96	37.8	46.8	46.2				
Ni	4.15	3.01	5.46	3.36	144.1	183	222	141	203	144	141
Sc	9.55	9.49	8.92	9.65	25.2	30.6	35.1	40.6	44.3	43.1	40.6
V	36.9	39.4	34.0	36.1	137.8	179.1	217	141	203	144	141
Zr	118	126	114	72.6	35.1	31.0	16.6	2.80	7.67	4.51	2.80
Hf	4.17	4.47	4.03	2.54	1.48	1.42	0.76	0.14	0.31	0.20	0.14
Ta	0.15	0.16	0.14	0.07	0.03	0.03	0.05	0.24	0.24	0.44	0.24
Sr	78.2	146	110	109	204	115	104	138	130	70.1	138
Ba	11.6	10.0	10.5	22.8	27.1	30.3	26.1	8.85	11.9	9.19	8.85
Nb	1.65	1.74	1.58	0.88	0.40	0.37	0.42	0.62	0.72	1.11	0.62
Cs	0.10	0.06	0.15	0.40	0.08	0.33	0.23	0.19	0.14	0.04	0.19
Ga	8.70	11.9	8.18	9.42	12.1	11.3	12.3	27.2	27.9	28.0	27.2
Pb	1.06	1.41	0.76	1.03	2.48	1.07	0.62	0.19	0.14	0.041	0.19
Th	0.67	0.72	0.64	0.62	0.18	0.07	0.29	0.09	0.07	0.09	0.09
U	0.57	0.60	0.51	0.44	0.11	0.05	0.04	0.01	0.02	0.01	0.01
Y	23.8	27.9	23.9	14.8	13.2	15.24	17	4.85	9.03	6.01	4.74
La	3.04	3.36	3.21	2.08	1.61	0.74	0.97	0.16	0.34	0.16	0.34
Ce	9.24	10.1	9.53	6.87	2.41	1.99	2.28	0.41	1.03	0.48	0.65
Pr	1.24	1.37	1.29	0.80	0.59	0.41	0.49	0.09	0.24	0.11	0.12
Nd	5.84	6.63	6.27	3.68	3.52	2.49	2.96	0.58	1.46	0.72	0.65
Sm	1.81	2.06	1.93	1.23	1.29	1.2	1.36	0.29	0.61	0.38	0.30
Eu	0.30	0.37	0.32	0.28	0.51	0.47	0.66	0.23	0.33	0.19	0.17
Gd	2.35	2.78	2.54	1.53	1.7	1.82	2.27	0.40	0.82	0.50	0.40
Tb	0.46	0.56	0.49	0.31	0.38	0.41	0.45	0.11	0.22	0.14	0.11
Dy	3.39	4.02	3.50	2.17	2.73	3.01	3.14	0.83	1.56	1.07	0.79
Ho	0.76	0.91	0.81	0.50	0.6	0.68	0.66	0.18	0.35	0.23	0.18
Er	2.47	2.94	2.58	1.62	1.54	1.77	1.96	0.56	1.03	0.69	0.53
Tm	0.44	0.50	0.43	0.27	0.29	0.33	0.30	0.1	0.19	0.12	0.09
Yb	3.08	3.56	3.07	1.96	1.73	2.09	2.03	0.61	1.18	0.77	0.59
Lu	0.52	0.61	0.53	0.32	0.23	0.28	0.30	0.1	0.18	0.12	0.09
ΣREE	34.94	39.77	36.50	23.62	19.13	17.67	19.83	4.65	9.54	5.68	5.02
LREE/HREE	1.59	1.50	1.62	1.72	1.08	0.70	0.78	0.61	0.73	0.56	0.80
$(La/Yb)_N$	0.71	0.68	0.75	0.76	0.63	0.24	0.32	0.18	0.19	0.14	0.39
δEu	0.44	0.47	0.44	0.62	1.05	0.97	1.14	2.06	1.43	1.33	1.5

peridotite of a suprasubduction zone type (SSZ-type) ophiolite, and date the timing of subduction (Sorensen and Grossman, 1989; Li and Li, 2003a; Yoshikawa and Ozawa, 2007). (4) Obduction-type plagiogranites form during the obduction of ophiolites by partial melting of sediments in the lower subducting marginal basin. This type of plagiogranite typically intrudes mantle peridotite of the lower part of the ophiolite sequence, and its age corresponds to the timing of the obduction and emplacement of oceanic crust (Pearce, 1989; Cox et al., 1999; Skjerlie et al., 2000; Whitehead et al., 2000).

The formation environment/mechanisms and source(s) of silicic rocks determine their spatial occurrence and geochemical characteristics (Li Xianwu and Li Xianhua, 2003; Li and Li, 2003; Koepke et al., 2004, 2007; Yoshikawa and Ozawa, 2007; Skjerlie et al., 2000; Whitehead et al., 2000; Freund et al., 2014). The Diyanmiao plagiogranites occur in the upper pillow basalts of the ophiolite sequence as irregular veins and small-scale bodies, which is consistent with the field occurrence of fractionation-type plagiogranites, and contrasts with the occurrence of shearing-, subduction-, and obduction-type plagiogranites. In addition, plagiogranites in the Diyanmiao ophiolite are

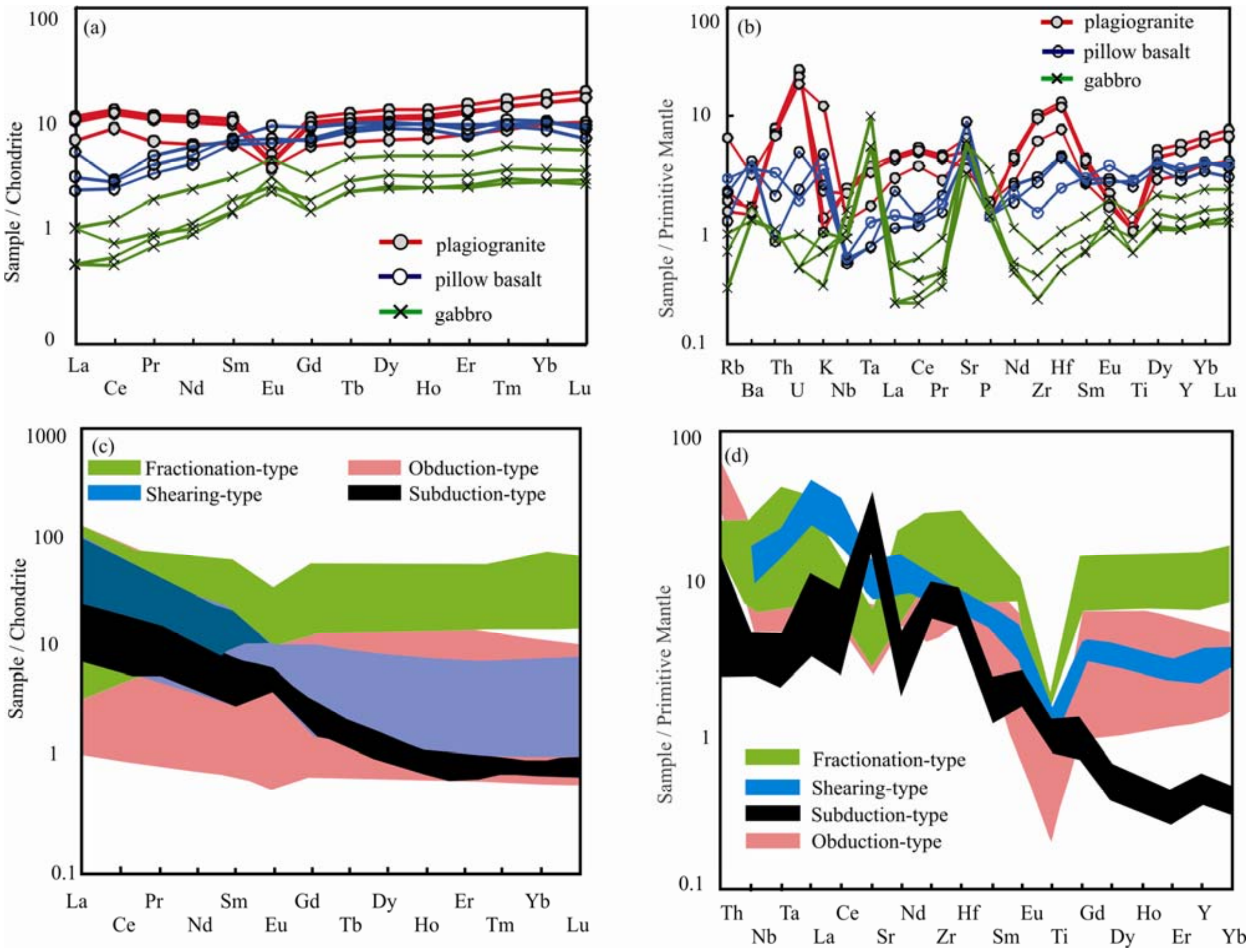

Fig. 6. Chondrite-normalized REE distribution patterns (normalizing values after Boynton, 1984) (a) and Primitive mantle-normalized trace element spider diagram (normalizing values after Sun and McDonough, 1989) (b) of the plagiogranite, pillow basalt and gabbro in Diyanmiao ophiolite, REE patterns (c) and trace elements spidegrams (d) (modified from Li and Li, 2003; Gao Xiaofeng et al., 2011) of different types of granitoids within ophiolites.

characterized by relatively low Al_2O_3 (11.9–13.30wt%) concentrations that are comparable with fractionation- and shearing-type plagiogranites (Al_2O_3<15wt%) (Pedersen and Malpas, 1984; Flagler and Spray, 1991; Li Xianwu and Li Xianhua, 2003; Gao XiaoFeng et al., 2011) and different from subduction-type (Al_2O_3>15wt%) and obduction-type plagiogranites (highly variable Al_2O_3). Plagiogranites in the Diyanmiao ophiolite are also characterized by high Na_2O (4.52–6.06wt%), very low K_2O (0.03–0.07wt%), and high Na_2O/K_2O ratios (average=105.3) that are similar to fractionation-type plagiogranites (Na_2O/K_2O>3–5) and higher than shearing-type plagiogranites (Na_2O/K_2O>1) (Pedersen and Malpas,1984; Flagler and Spray,1991; Li and Li, 2003; Gao et al., 2011). These rocks have low ∑REE (23.62–39.77 ppm), small negative Eu anomalies (δEu=0.44–0.62), and flat chondrite-normalized REE patterns ($(La/Yb)_N$=0.68–0.76; Fig. 6a), similar to fractionation-type plagiogranites and slightly different from shearing-type plagiogranites (minor light REE enrichment with a wide range of δEu) and distinctly different from subduction-type (light REE enriched and heavy REE depleted) and obduction-type plagiogranites (LREE enriched) (Fig. 6c) (Pedersen and Malpas, 1984; Flagler and Spray, 1991; Li and Li, 2003; Gao XiaoFeng et al., 2011). Primitive-mantle-normalized trace element patterns of the Diyanmiao plagiogranites have overall flat patterns (Fig. 6b) with obvious P and Ti anomalies, consistent with fractionation-type plagiogranites (Fig. 6d), but are slightly different from shearing-type plagiogranites (gently right-dipping patterns), and clearly distinct from subduction-type (marked Sr anomaly and steeply right-dipping patterns) and obduction-type plagiogranites (highly variable right-dipping patterns) (Fig. 6d). The chondrite-normalized REE patterns of the plagiogranites are similar to those of the gabbros and pillow basalts (Table 3; Fig. 6a). The REE concentrations increase from the gabbros to the pillow basalts and to the plagiogranites (Fig. 6a), which is consistent with progressive fractional crystallization and differentiation. The plagiogranites have complementary Eu anomalies to the gabbros (Fig. 6a), which can be interpreted as reflecting magma crystallization resulting in the formation of gabbros with positive Eu anomalies and a residual melt with negative Eu anomalies (Tang et al., 2007).

Brophy (2009) and Brophy and Pu (2012) summarized the geochemical characteristics of fractionation- and shearing-type plagiogranites in global examples of ophiolites. Fractionation-type plagiogranites have steadily increasing La and Yb abundances with increasing SiO_2, with total REE abundances being significantly higher than those in associated mafic rocks (Fig. 7). In contrast, shearing-type plagiogranites have constant or decreasing La and constant Yb abundances with increasing SiO_2, with ∑REE being lower than those in associated mafic rocks (Fig. 7). As shown in Table 3, the average ∑REE of the plagiogranites and associated pillow basalts and gabbros are 6.22, 18.15, and 33.7ppm, respectively, showing that the ∑REE increase with increasing SiO_2. In addition, the La and Yb contents increase with increasing SiO_2 (Fig. 7). These features suggest that plagiogranites in the Diyanmiao ophiolite are fractionation-type plagiogranites.

On a Th/Yb–Ta/Yb plot (Fig. 8a), data for the plagiogranites and pillow basalts plot within the tholeiitic series field. On a Hf/3–Th–Ta diagram (Fig. 8b), data for the plagiogranites and pillow basalts plot within the island arc tholeiite (IAT) field. On a Th/Yb–Ta/Yb diagram (Fig. 8c), data for six samples plot within the oceanic island arc field, with one sample lying at the boundary of the oceanic island arc field. These characteristics suggest that both the pillow basalts and plagiogranites in the Diyanmiao ophiolite formed in an incipient oceanic arc setting (Weaver et al., 1979; Hawkine, 2003; Dilek and Fumes, 2009, 2014) and are the products of submarine eruptions and the differentiation of oceanic basaltic magmas. In an R_1–R_2 diagram (Fig. 8d), data for the plagiogranite samples plot within the mantle plagiogranite field, again suggesting that the plagiogranites formed by the differentiation of oceanic basalts.

In summary, the available geological and geochemical data suggest that the plagiogranites are leucocratic or silicic end-member rocks in the Diyanmiao ophiolite, are part of the oceanic crust, and are fractionation-type oceanic plagiogranites formed by the fractional crystallization of mafic magmas during gabbro formation. Such plagiogranites have been reported from Oman, Troodos and other SSZ-type ophiolites (Pearce et al., 1984; Rollinson, 2009; Freund et al., 2014).

5.2 Age of the Diyanmiao ophiolite and its implications

Although ophiolites are dominated by mafic and ultramafic rocks, minor granitoids (generally<10% of the rock mass) within these sequences provide important information about the ophiolite origins, including robust ages and evidence for the evolution of these segments of oceanic crust (Jian Ping et al., 2003b; Li Xianwu and Li Xianhua, 2003; Wang Cunzhi et al., 2011).

The Diyanmiao ophiolite is considered to be part of the Erenhot–Hegenshan ophiolite belt, and it can be compared with other ophiolites in the Erenhot–Hegenshan ophiolite.

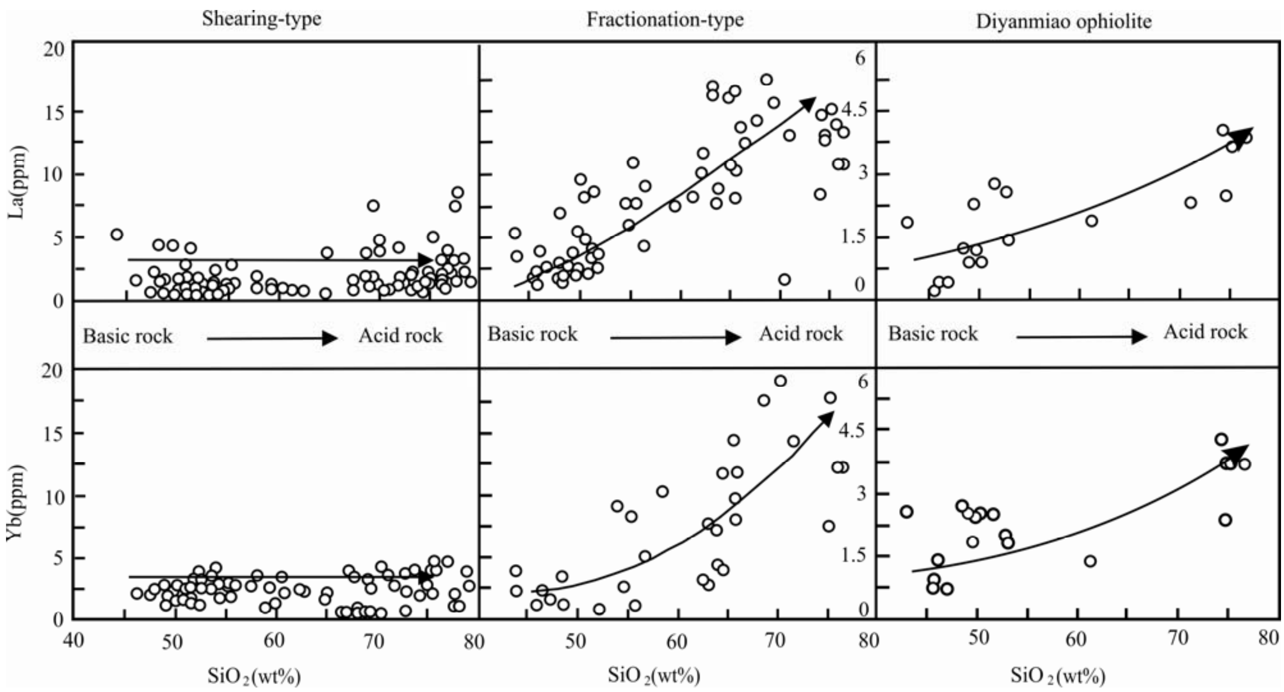

Fig. 7. La–SiO_2 and Yb–SiO_2 (after Brophy, 2009) plots of plagiogranite, gabbro and pillow basalt in the Diyanmiao ophiolite.

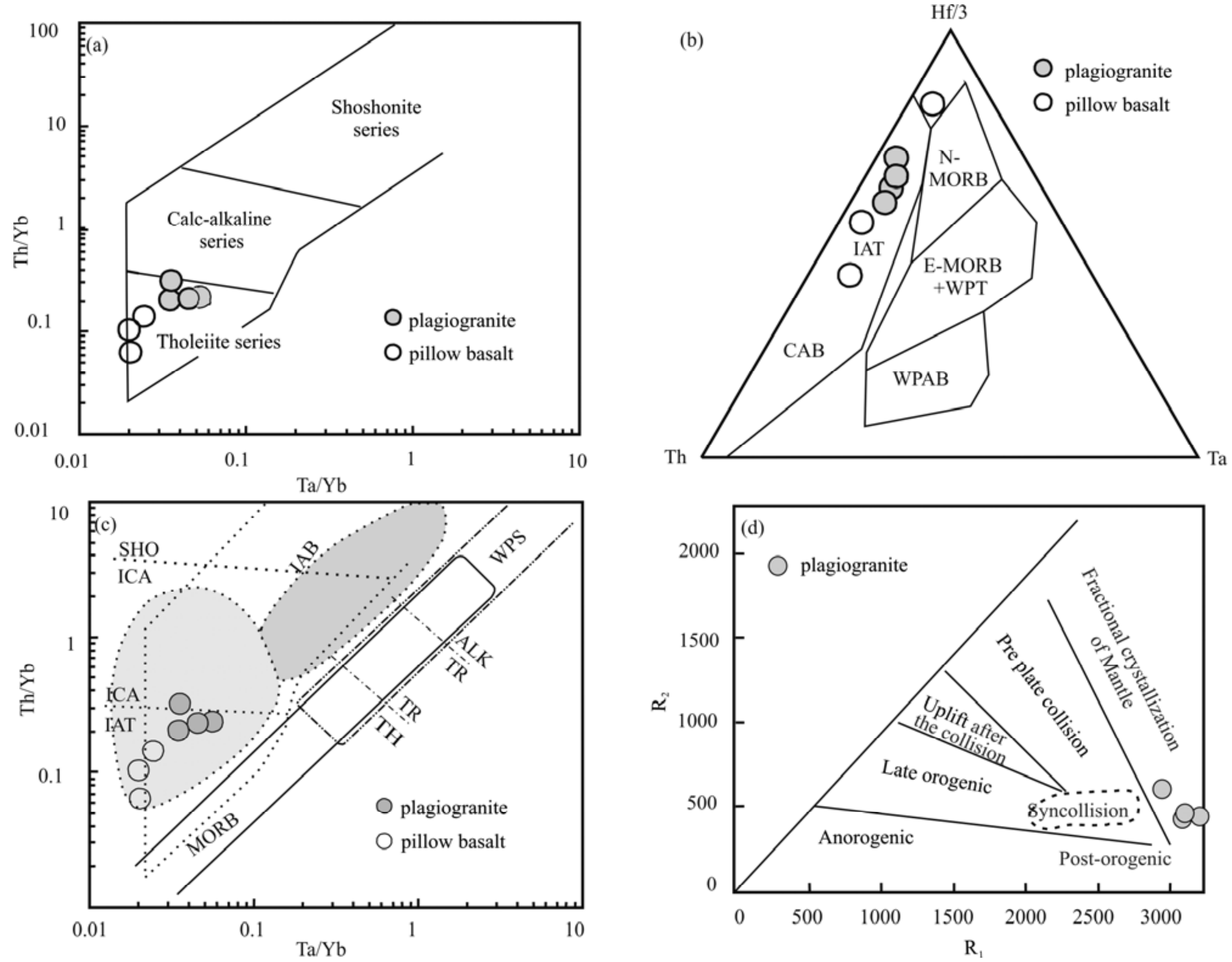

Fig. 8. Th/Yb-Ta/Yb classification diagrams (a), Hf/3–Th–Ta diagram (after Wood, 1980) (b) and Th/Yb–Ta/Yb tectonic discriminant diagrams (after Pearce, 1982) (c) of the plagiogranite and pillow basalt in the Diyanmiao ophiolite, and R_2–R_1 tectonic discriminant diagram of the plagiogranite in the Diyanmiao ophiolite (after De La Rache et al., 1980; Hong et al., 1996).

The age of the Erenhot–Hegenshan ophiolite is controversial, which has implications for understanding the Paleozoic tectonic evolution of the southeastern Altaids. In particular, fossil ages are not consistent with isotopic ages (Miao et al., 2008; Jian et al., 2012). Fossil ages of the Erenhot–Hegenshan ophiolite are mainly from fossils in overlying deep-sea sedimentary rocks (e.g., cherts and limestones), but the relationship between the sedimentary rocks and ophiolite is unclear. Zircon U–Pb dating of magmatic rocks in ophiolites can provide useful age constraints, but this approach is challenging because such rocks rarely contain zircons and often contain a composite magmatic and xenocrystic zircon population (Jian et al., 2012; Koglin et al., 2009; Liati et al., 2003; Freund et al., 2014). Fractionation-type plagiogranites are ideal for precise dating of ophiolite formation (Freund et al., 2014). Given that fractionation-type plagiogranites typically represent the latest additions to the ophiolitic crust, their crystallization ages reflect the last stages of ophiolite formation (e.g., Robinson et al., 2008; Rioux et al., 2012; Grimes et al., 2013).

Our new LA–ICP–MS U–Pb age data for fractionation-type plagiogranites in the Diyanmiao ophiolite yield consistent ages of 328.6±2.1 and 327.1±2.1Ma (i.e., early Carboniferous), which constrain the timing of the last stages of ophiolite formation (Rioux et al., 2012). These ages are similar to U–Pb ages of 354±7Ma reported for microgabbro and 333±4Ma for plagiogranite in the Hegenshan ophiolite (Jian et al., 2012), 354±4.5 and 353±3.7Ma reported for gabbro and 345±5.5Ma for plagiogranite in the eastern Erenhot ophiolite (Zhang et al., 2015b), 343±7Ma reported for plagiogranite in the Jiaoqier ophiolite (Miao et al., 2007), and 315±6.2Ma reported for gabbros from the Meilaotewula ophiolite (Li Yingjie et al., 2015) (Fig. 1a). These age data confirm the occurrence of a vast Carboniferous ophiolitic complex belt from Erenhot to Hegenshan.

The early Carboniferous Diyanmiao ophiolite comprises a relative complete ophiolite sequence within the Erenhot–Hegenshan ophiolite belt. It is structurally located between the early Permian Shoushangou formation and Dashizhai formation, which indicates that the ophiolite was tectonically emplaced after the early Permian. The Diyanmiao ophiolite thus provides important information about the rocks, original ophiolite sequence, spatial distribution, formation environment, emplacement age, and tectonic evolution of the Erenhot–Hegenshan ophiolite belt. The Diyanmiao ophiolite represents an important north-directed subduction event of Paleo-Asian oceanic crust beneath the southern margin of the Siberian plate, and provides key evidence regarding the location and age of the collision between oceanic and continental crust.

6 Conclusions

(1) Geological, petrological, and geochemical characteristics of plagiogranites in the Diyanmiao ophiolite indicate that they formed by crystal fractionation from a tholeiitic magma during oceanic spreading, representing a silicic end-member of the Diyanmiao ophiolite and paleo-oceanic crust.

(2) LA–ICP–MS U–Pb zircon dating of the plagiogranites yielded ages of 328.6±2.1 and 327.1±2.1Ma, indicating an early Carboniferous age for the Diyanmiao ophiolite.

(3) The discovery of fractionation-type plagiogranites in the Diyanmiao ophiolite and their ages provide important petrological and age constraints on the formation and evolution of the Erenhot–Hegenshan oceanic basin in the Paleo-Asian Ocean.

Acknowledgments

This study was financially supported by the National Natural Science Foundation of China (41502211), the China Geological Survey (1212011120701, 1212011120711, 12120114064201, DD20160041) and the Research Fund for the Doctoral Program of Hebei GEO University (BQ2017052). We thank Gu Yongchang, Liu Yongshun, Xin Houtian, and Zhou Hongying of Tianjin Institute of Geology and Mineral Resources, China Geological Survey, for their helpful suggestions and data.

Manuscript received Oct. 24, 2017
accepted Jan. 13, 2018
edited by Liu Lian

References

Amri, I., Benoit, M., and Ceuleneer, G., 1996. Tectonic setting for the genesis of oceanic plagiogranites: Evidence form a paleo-spreading structure in the Oman ophiolite. *Earth and Planetary Science Letters*, 139(1–2): 177–194.

Andersen, T., 2002. Correction of commen lead U-Pb analyses that do not report ^{204}Pb. *Chemical Geology*, 192: 59–79, doi: 10.1016/S0009-2541(02)00195-X.

Badarch, G., Gunningham, W.D., and Windley, B.F. 2002. A new terrane subdivision for Mongolia: implications for the Phanerozoic crustal growth of Central Asia. *Journal of Asian Earth Sciences*, 21: 87–110.

Baines, A.G., Cheadle, M.J., John, B.E., Grimes, C.B., Schwartz, J.J., and Wooden, J.L., 2009. SHRIMP Pb/U zircon ales constrain gabbroic crustal accretion at Atlantis Bank on the ultraslow-spreading Southwest Indian Ridge. *Earth and Planetary Science Letters*, 287: 540–550.

Bao Zhiwei, Chen Shenhuang and Zhang Zhentang., 1994. Study on REE and Sm-Nd isotopes of Hegenshan ophiolite, Inner Mongolia. *Geochimica*, 23(4): 339–349 (in Chinese with English abstract).

Bébien, J., Dautaj, N., Shallo, M., Turku, I., and Barbarin, B., 1997. Diversity of ophiolitic plagiogranites: The Albanian example. Comptes Rendus de 1'Academia des Sciences-Series-IIA *Earth and Planetary Science*, 324(11): 875–882.

Bebout, G.E., and Barton, M.D., 1993. Metasomatism during subduction Products and possible paths in the Catalina schist, California. *Chemical Geology*, 108(1–4): 61–92.

Belousova, E.A., Griffin, W.L., O'Reilly, S.Y., and Fisher, N.L., 2002. Igneous zircon: trace element composition as an indicator of source rock type. *Contributions to Mineralogy and Petrology*, 143(5): 602–622.

Buchan, C., Pfander, J., KrÖner, A., Brewer, T.S., Tomurtogoo, O., Tomurhuu, D., Cunningham, D., and Windley, B.F., 2002. Timing of accretion and collisional deformation in the Central Asian Orogenic Belt: Implications of granite geochronology in the Bayankhongor Ophiolite Zone. *Chemical Geology*, 192 (1–2): 23–45.

Brophy, J.G., 2009. La-SiO_2 and Yb-SiO_2 systematics in mid-ocean ridge magmas: Implications for the origin of oceanic plagiogranite. *Contributions to Mineralogy and Petrology*, 158(1): 99–111.

Brophy, J.G., and Pu, X.F., 2012. Rare earth element-SiO_2 systematics of mid-ocean ride plagiogranites and host gabbros from the Fournier oceanic fragment, New Brunswick, Canada: A field evaluation of some model predictions. *Contributions to Mineralogy and Petrology*, 164(2): 191–204.

Coleman, R.G., and Peterman, Z.E., 1975. Oceanic plagiogranite. *Journal of Geophysical Research Atmospheres*, 80: 1099–1108.

Cheng Yinhang, Zhang Tianfu, Li Yanfeng, Li Min, Niu Wenchao, Teng Xuejian, DUANuan Lianfeng, Liu Yang, Du Yelong and Hu Xiaojia, 2016. Discovery of the early Permian ultramafic rock in Dong Ujimqi, Inner Mongolia and its tectonic Implications. *Acta Geologica Sinica*, 90(01): 115–125 (in Chinese with English abstract).

Claoue-long, J.C., Compston, W., Roberts, J., and Fanning, C.M., 1995. Two carboniferous ages: A comparison of SHRIMP zircon dating with conventional zircon ages and ^{40}Ar/^{39}Ar analysis. In: Berggren, W.A., Kent, D.V., Aubry, M.P., et al, (eds). Geochronology, Time Scales and Global Stratigraphic Correlation. *SEPM Special Publication*, 4: 3–31.

Cox, J., Searle, M., and Pedersen, R., 1999. The petrogenesis of leucogranitic dykes intruding the northern Semail ophiolite, United Arab Emirates: field relationships, geochemistry and

Sr/Nd isotope systematics. *Contributions to Mineralogy & Petrology*, 137(3): 267–287.

David, C.G., William, P.L., and Hans, G.A.L., 1981. Petrology and geochemistry of plagiogranite in the Canyon Mountain ophiolite, Oregon. *Contributions to Mineralogy & Petrology*, 77: 82–89.

Dang Zhicai, Li Junjianl, Fu Chao, Tang Wenlong, Liu Yue, Zhao Zelin, Wu Xingyuan and Sun Hongwei, 2018. Geochronological, Mineralogical and Lithogeochemical Studies of the Kebu Mafic-ultramafic Intrusion in Urad Middle Banner, Inner Mongolia. *Acta Geologica Sinica*, 92 (2): 278–297 (in Chinese with English abstract).

De la Roche, H., Leterrier, J., Grandclaude, P., and Marchal, M., 1980. A classification of volcanic and plutonic rocks using R_1R_2-diagram and major-element analyses-Its relationships with current nomenclature. *Chemical Geology*, 29(1–4): 183–210.

Dilek, Y., and Furnes, H., 2009. Structure and geochemistry of Tethyan ophiolites and then petrogenesis in subduction rollback systems. *Lithos*, 113: 1–20.

Dilek, Y., and Furnes, H., 2014. Ophiolites and their origins. *Elements*, 10: 93–100.

Flagler, P.A., and Spray, J.G., 1991. Generation of plagiogranite by amphibolite anatexis in oceanic shear zones. *Geology*, 19 (1): 70–73.

Floyd, P.A., Yaliniz, M.K., and Goncuoglu, M.C., 1998. Geochemistry and petrogenesis of intrusive and extrusive ophiolitic plagiogranites, Central Anatolian Crystalline Complex, Turkey. *Lithos*, 42: 225–241.

France, L., Koepke, J., Ildefonse, B., Cichy, S.B., and Deschamps, F., 2010. Hydrous partial melting in the sheeted dike complex at fast spreading ridges: Experimental and natural observations. *Contributions to Mineralogy and Petrology*, 160(5): 683–704.

Freund, S., Haase, K., Keith, M., Beier, C., and Garbe-SchÖnberg, D., 2014. Constraints on the formation of geochemically variable plagiogranite intrusions in the Troodos Ophiolite, Cyprus. *Contributions to Mineralogy & Petrology*, 167: 1–22.

Furnes, H., and Dilek, Y., 2017. Geochemical characterization and petrogenesis of intermediate to silicic rocks in ophiolites: A global synthesis. *Earth-Science Reviews*, 166: 1–37.

Gai Yongsheng, Liu Liang, Kang Lei, Yang Wenqiang, Liao Xiaoying and Wang Yawei., 2015. The origin and geologic significance of plagiogranite in ophiolite belt at North Altyn Tagh. *Acta Petrologica Sinica*, 31(9): 2549–2565 (in Chinese with English abstract).

Gao Xiaofeng, Xiao Peixi, Guo Lei, Dong Zengchan and Xi Rengang, 2011. Opening of an early Paleozoic limited oceanic basin in the northern Altyn area: Constraints from plagiogranites in the Hongliugou-Lapeiquan ophiolitic melange. *Science in China* (Earth Science), 54(12): 1871–1879.

Gerlach, D.C., Leaman, W.P., and Lallemant, H.G.A., 1981. Petrology and geochemistry of plagiogranite in the Canyon Mountain ophiolite Oregon. *Contributions to Mineralogy and Petrology*, 77(1): 82–92.

Grimes, C.B., John, B.E., Cheadle, M.J., Mazdab, F.K., Wooden, J.L. Swapp, S., and Schwartz, J.J., 2009. On the occurrence, trace element geochemistry, and crystallization history of zircon from in situ ocean lithosphere. *Contributions to Mineralogy and Petrology*, 158(6): 757–783.

Grimes, C.B., Ushikubo, T., Kozdon, R., and Valley, J.W., 2013. Perspectives on the origin of plagiogranite in ophiolites from oxygen isotopes in zircon. *Lithos*, 179(5): 48–66

Hawkins, J.W., 2003. Geology of supra-subduction zones-Implications for the origin of ophiolites. *Geological Society of America Special Paper*, 373: 227–268.

Hou, K.J., Li, Y.H., and Tian, Y.R, 2009. In situ U-Pb zircon dating using laser ablation-multi ion counting-ICP-MS. *Mineral Deposits*, 28(4): 481–492 (in Chinese with English abstract).

Huang Bo, Fu Dong, Li Shucai, Ge Mengchun and Zhou Wenxiao., 2016. The age and tectonic implications of the Hegenshan ophiolite in Inner Mongolia. *Acta Petrologica Sinica*, 32(1): 158–176 (in Chinese with English abstract).

Jackson, S.E., Pearson, N.J., Griffin, W.L., and Belousova, E.A., 2004. The application of laser ablation-inductively coupled plasma-mass spectrometry to in situ U-Pb zircon geochronology. *Chemical Geology*, 211(1): 47–69.

Jafri, S.H., Charan, S.N., and Govil, P.K., 1995. Plagiogranite from the Andaman ophiolite belt, Bay of Bengal, India. *Journal of the Geological Society*, 152(4): 681–687.

Jahn, B.M., Wu, F.Y., and Chen, B., 2000. Granitoids of the Central Asian Orogenic Belt and continental growth in the Phanerozoic. Transactions of the Royal Society of Edinburgh: *Earth Sciences*, 91(1–2): 181–193.

Jahn, B.M., Windley, B., Natal'in, B., and Dobretsov, N., 2004. Phanerozoic continental growth in Central Asia. *Journal of Asian Earth Sciences*, 23(5): 599–603.

Jian Ping, Liu Dunyi and Sun Xiaomeng, 2003a. SHRIMP dating of Carboniferous Jinshajiang ophiolite in western Yunnan and Sichuan: Geochronological constraints on the evolution of the Paleo-Tethys oceanic crust. *Acta Geologica Sinica*, 77(2): 217–228(in Chinese with English abstract).

Jian Ping, Liu Dunyi, Zhang Qi, Zhang Fuqin, Shi Yuruo, Shi Guanghuai, Zhang Lvqiao and Tao Hua, 2003b. SHRIMP dating of ophiolite and leucocratic rocks within ophiolite. *Earth Science Frontiers*, 10(4): 439–456 (in Chinese with English abstract).

Jian, P., Liu, D., KrÖner, A., Windley, B.F., Shi, Y., Zhang, F., Shi, G., Miao, L., Zhang, W., Zhang, Q., Zhang, L., and Ren, J., 2008. Time scale of an early to mid-Paleozoic orogenic cycle of the long-lived Central Asian Orogenic Belt, Inner Mongolia of China: implications for continental growth. *Lithos*, 101(3): 233–259.

Jian, P., Liu, D., KrÖner, A., Windley, B.F., Shi, Y., Zhang, W., Zhang, F., Miao, L., Zhang, L., and Tomurhuu, D., 2010. Evolution of a Permian intraoceanic arc-trench system in the Solonker suture zone, Central Asian Orogenic Belt, China and Mongolia. *Lithos*, 118(1–2): 169–190.

Jian, P., KrÖner, A., Windley, B.F., Shi, Y.R., Zhang, W., Zhang, L.Q., and Yang, W.R., 2012. Carboniferous and Cretaceous mafic-ultramafic massifs in Inner Mongolia (China): A SHRIMP zircon and geochemical study of the previously presumed integral "Hegenshan ophiolite". *Lithos*, 142–143: 48–66.

Jiang, T., Gao, J., Klemd, R., Qian, Q., Zhang, X., Wang, X., Tan, Z., and Zhu, Z., 2015. Genetically and geochronologically contrasting plagiogranites in South

Central Tianshan ophiolitic melange: Implications for the breakup of Rodinia and subduction zone processes. *Journal of Asian Earth Sciences*, 113: 266–281.

Kang Lei, Xiao Peixi, Gao Xiaofeng, Wang Chao, Yang Zaichao and Xi Rengang, 2015. Geochemical characteristics, petrogenesis and tectonic setting of Oceanic plagiogranites belt in the northwestern margin of western Kunlun. *Acta Petrologica Sinica*, 31(9): 2566–2582 (in Chinese with English abstract).

Kang Jianli, Xiao Zhibin, Wang Huichu, Chu Hang, Ren Yunwei, Liu Huan, Gao Zhirui and Sun Yiwei. 2016. Late Paleozoic Subduction of the Paleo-Asian Ocean Geochronological and Geochemical Evidence from the Meta-basic Volcanics of Xilinhot, Inner Mongolia. *Acta Geologica Sinica*, 90(2): 383–397 (in Chinese with English abstract).

Khain, E.V., Bibikova, E.V., Salnikova, E.B., KrÖner, A., Gibsher, A.S., Didenko, A.N., Degtyarev, K.E., and Fedotova, A.A., 2003. The Palaeo-Asian ocean in the Neoproterozoic and early Palaeozoic: new geochronologic data and palaeotectonic reconstructions. *Precambrian Research*, 122(1–4): 329–358.

Koepke, J., Feig, S.T., Snow, J., and Freise, M., 2004. Petrogenesis of oceanic plagiogranites by partial melting of gabbros: an experimental study. *Contributions to Mineralogy & Petrology*, 146: 414–432.

Koepke, J., Berndt, J., Feig, S.T., and Holtz, F., 2007. The formation of SiO_2 -rich melts within the deep oceanic crust by hydrous partial melting of gabbros. *Contributions to Mineralogy and Petrology*, 153(1): 67–84.

Kovalenko, V.I., Yarmolyuk, V.V., Kovach, V.P., Kotov, A.B., Kozakov, I.K., Salnikova, E.B., and Larin, A.M., 2004. Isotope provinces, mechanisms of generation and sources of the continental crust in the Central Asian mobile belt: Geological and isotopic evidence. *Journal of Asian Earth Sciences*, 23(5): 605–627.

KrÖner, A., Hegner, E., Lehmann, B., Heinhorst, J., Wingate, M.T.D., Liu, D.Y., and Ermelov, P., 2008. Palaeozoic arc magmatism in the Central Asian Orogenic Belt of Kazakhstan: SHRIMP zircon ales and whole- rock Nd isotopic systematics. *Journal of Asian Earth Sciences*, 32(2–4): 118–130.

KrÖner, A., Demoux, A., Zack, T., Rojas-Agramonte, Y., Jian, P., Tomurhuu, D., and Barth, M., 2011. Zircon ages for a felsic volcanic rock and arc-related early Palaeozoic sediments on the margin of the Baydrag microcontinent, central Asian orogenic belt, Mongolia. *Journal of Asian Earth Sciences*, 42: 1008–1017.

KrÖner, A., Kovach, V., Aledeiev, D., Wang, K.L., Wong, J., Degtyarev, K., and Kozakov, I., 2017. No excessive crustal growth in the Central Asian Orogenic Belt: Further evidence from field relationships and isotopic data. *Gondwana Research*, https://doi.org/10.1016/j.gr.2017.04.006

Le Maitre, R.W., 2009. Igneous Rocks: A Classification and Glossary of Terms. 2nd Edition. Cambridge: *Cambridge University Press*, 33–39.

Li, X.H., Faure, M., Lin, W., and Manatschal, G., 2013. New isotopic constraints on age and magma genesisi of an embryonic oceanic crust: The Chenaillet Ophiolite in the Western Alps. *Lithos*, 160–161: 283–291.

Liu Jiayi., 1983. The study and tectonic significance of ophiolites in Hegenshan region, Nei Mongol. In: CPPTNC Editorial Committee (ed.).Contributions for the Project of Plate Tectonics in Northern China (1).Shenyang: Shenyang Institute of Geology and Mineral Resources of Ministry, *Chinese Academy of Geological Sciences*, 117–135 (in Chinese).

Li Yingjie, Wang Jinfang, Li Hongyang, Liu Yucui, Dong Peipei, Liu Dewu and Bai Hui, 2012. Recognition of Diyanmiao ophiolite in Xi U jimqin banner, Inner Mongolia. *Acta Petrologica Sinica*, 28(4): 1282–1290 (in Chinese with English abstract).

Li Yingjie, Wang Jinfang, Li Hongyang, Dong Peipei, He Qiuli, Zhang Hongchen, and Song Peng, 2013. Geochemical characteristics of Baiyinbulage ophiolite in Xi U jimqin banner, Inner Mongolia. *Acta Petrologica Sinica*, 29(8): 2719–2730 (in Chinese with English abstract).

Li Yingjie, Wang Jinfang, Li Hongyang, and Dong Peipei, 2015. Recognition of Meilaotewula ophiolite in Xi U, jimqin banner, Inner Mongolia. *Acta Petrologica Sinica*, 31(5): 1461–1470 (in Chinese with English abstract).

Li YingJie, Wang JinFang, Wang Genhou, Li HongYang, and Dong PeiPei, 2018. Discovery and significance of the Dahate fore-arc basalts from Diyanmiao ophiolite in Inner Mongolia. *Acta Petrologica Sinica*, 34(02): 469–482 (in Chinese with English abstract).

Li,Y.J., Wang G.H., Santosh, M., Wang, J.F., Peipei Dong, P.P., and Li H.Y., 2018. Supra-subduction zone ophiolites from Inner Mongolia, North China: Implications for the tectonic history of the southeastern Central Asian Orogenic Belt. Gondwana Research, https://doi.org/10.1016/j.gr.2018.02.018

Li, W.X., and Li, X.H., 2003. Adakitic granites within the NE Jiangxi ophiolites, South China: Geochemical and Nd isotopic evidence. *Precambrian Research*, 122(1–4): 29–44.

Li Wuxian and Li Xianhua, 2003. Rock types and tectonic significance of the granitoids rocks within ophiolites. *Advance in Earth Sciences,* 18(3): 392–397 (in Chinese with English abstract).

Liang, R., 1991. The characteristics of the ophiolite sequences and its rock associations in central and eastern Inner Mongolia. In: Ishii, K., Liu, X., Ichikawa, K., and Huang, B. (Eds.), *Pre-Jurassic Geology of Inner Mongolia, China*. Osaka: China-Japan Cooperative Research Group, 65–84.

Liang Rixuan, 1994. The Features of ophiolites in the central sector of Inner Mongolia and its geological significance. *Geological Bulletin of China,* (1): 37–45 (in Chinese with English abstract).

Liu Jiayi, 1983. *The study and tectonic significance of ophiolites in Hegenshan region, Nei Mongol*. In: CPPTNC Editorial Committee (ed.).Contributions for the Project of Plate Tectonics in Northern China (1). Shenyang: Shenyang Institute of Geology and Mineral Resources of Ministry, Chinese Academy of Geological Sciences, 117–135 (in Chinese).

Liu, Y.S., Gao, S., Hu, Z.C., Gao, C.G., Zong, K.Q., and Wang, D.B., 2009. Continental and oceanic crust recycling-induced melt-peridotite interactions in the Trans-North China Orogen: U–Pb dating, Hf isotopes and trace elements in zircons from mantle xenoliths. *Journal of Petrology*, 51(1–2): 537–571.

Liu, Y.S., Hu, Z.C., Gao, S., Detlef, G., Xu, J., Gao, C.G., and Chen, H.H., 2008. In situ analysis of major and trace elements of anhydrous minerals by LA-ICP-MS without applying an internal standard. *Chemical Geology*, 257(1–2): 34–43.

Ludwig, K.R., 1991. Isotope: a plotting and regression program for radiogenic-isotope data. *US Geological Survey Open-File Report*, 39: 91–445.

Ludwig, K.R., 2003. *User's Manual for Isoplot 3.00.* Berkeley: Berkeley Geochronological Center Special Publication, 4: 71.

Miao, L.C., Fan, W.M., Liu, D.Y., Zhang, F.Q., Shi, Y.R, and Guo, F., 2008. Geochronology and geochemistry of the Hegenshan ophiolitic complex: Implications for late-stage tectonic evolution of the Inner Mongolia-Daxinganling Orogenic Belt, China. *Journal of Asian Earth Sciences*, 32(5–6): 348–370.

Nozaka, T., and Liu, Y., 2002. Petrology of the Hegenshan ophiolite and its implication for the tectonic evolution of northern China. *Earth and Planetary Science Letters*, 202(1): 89–104.

Pearce, J.A., 1982. Trace element characteristics of lavas from destructive plate boundaries. *Andesites*, 528–548.

Pearce, J.A., Lippard, S.J., and Roberts, S., 1984. Characteristics and tectonic significance of supra-subduction zone ophiolites. In: Kokelaar BP and Howells MF (eds.). Marginal basin geology. *Geological Society of London Special Publication*, 16: 77–94.

Pearce, J.A., 1989. High T/P metamorphism and granite genesis beneath ophiolite thrust sheets. *Ofioliti*, 14: 195–211.

Pedersen, R.B., and Malpas, J., 1984. The origin of oceanic plagiogranites from the Karmoy ophiolite, western Norway. *Contributions to Mineralogy and Petrology*, 88(1–2): 36–52.

Peters, T., and Kamber, B.S., 1994. Peraluminous, potassium-rich granitoids in the Semail ophiolite. *Contributions to Mineralogy and Petrology*, 118(3): 229–238.

Pidgeon, R.T., Nemchin, A.A., and Hitches, G.J., 1998. Internal structures of zircons from Archaean granites from the Darling Range batholith: Implications for zircon stability and the interpretation of zircon U-Pb ages. *Contributions to Mineralogy and Petrology*, 132(3): 288–299.

Rioux, M., Bowring, S., Kelemen P., Gordon, S., Dudás, F., and Miller, R., 2012. Rapid crustal accretion and magma assimilation in the Oman-U.A.E. ophiolite: High precision U-Pb zircon geochronology of the gabbroic crust. J*ournal of Geophysical Research Solid Earth*, 117(B7).

Robinson, P.T., Malpas, J., Dilek, Y., and Zhou, M.F., 2008. The significance of sheeted dike complexes in ophiolites. *GSA Today*, 18(11): 4–10 (1130/GSAT22A.1).

Rollinson, H., 2009. New models for the genesis of plagiogranites in the Oman ophiolite. *Lithos*, 112(3): 603-614.

Safonova, I., 2017. Juvenile versus recycled crust in the Central Asian Orogenic Belt: Implications from ocean plate stratigraphy, blueschist belts and intra-oceanic arcs. *Gondwana Research*, 47: 6–27.

Santosh, M., Teng, X.M., He, X.F., Tang, L., and Yang, Q.Y., 2016. Discovery of Neoarchean suprasubduction zone ophiolite suite from Yishui Complex in the North China Craton. *Gondwana Research*, 38: 1–27.

Scarrow, J.H., Pease, V., Fleutelot, C., and Dushin, V., 2001. The Late Neoproterozoic Enganepe ophiolite, Polar Urals, Russia: An extension of the Cadomian arc? *Precambrian Research*, 110(1–4): 255–275.

Schwartz, J. J., John, E.B., Cheadle, M.J., Miranda, E.A., Grimes, C.B., Wooden, J.L., and Dick, H.J.B., 2005. Dating the growt.h of oceanic crust at a slow-spreading ridge. *Science*, 310: 654–657.

Skjerlie, K.P., Pedersen, R.B., Wennberg, O.P., and De la Rosa, J., 2000. Volatile phase fluxed anatexis of metasediments during late Caledonian ophiolite obduction: evidence from the Sogneskollen Granitic Complex, west Norway. *Journal of the Geological Society*, 157: 1199–1213.

Searle, M.P., and Malpas, J., 1980. Structure and metamorphism of rocks beneath the Semail ophiolite of Oman and their significance in ophiolite obduction.*Transactions of the Royal Society of Edinburgh: Earth Sciences*, 71(4): 247–262.

ŞengÖr, A.M.C., Natal' in, B.A., and Rurtman, V.S. 1993. Evolution of the Altaid tectonic collage and Paleozoic crustal growth in Eurasia. *Nature*, 364(6435): 299–307.

ŞengÖr, A.M.C. and Natal'in, B.A., 1996. Paleotectonics of Asia: fragments of a synthesis. In: Yin, A., Harrison, M. (Eds.), T*he Tectonic Evolution of Asia. Cambridge University Press*, Cambridge, pp. 486–641.

Sorensen, S.S., and Grossman, J.N., 1989. Enrichment of trace elements in garnet amphibolites from a paleo-subduction zone: Catalina Schist, southern California. *Geochimica Et Cosmochimica Acta*, 53: 3155–3177.

Shao, J.A., 1989. Continental crust accretion and tectono-magmatic activity at the northern margin of the Sino-Korean plate. *Journal of Asian Earth Sciences*, 3: 57–62.

Sun, S.S., and McDonough, W.F., 1989. Chemical and isotopic systematics of oceanic basalts: Implications for mantle composition and processes. In: Sauders, A.D., and Norry, M.J. (eds.). Magmatism in the Ocean Basins. *Geological Society Special Publication*, 42: 313–345.

Tang Hongfeng, Su Yuping, Liu Congqiong, Hou Guangshun and Wang Yanbin, 2007. Zircon U-Pb age of the plagiogranite in Kalamaili belt, northern Xinjiang and its tectonic implications. *Geotectonica et Metallogenia*, 31(1): 110–117 (in Chinese with English abstract).

Tang, K.D., 1990. Tectonic development of Paleozoic foldbelts at the northern margin of the Sino-Korean Craton. *Tectonics*, 9(2): 249–260.

Tang, K., and Yan, Z. 1993. Regional metamorphism and tectonic evolution of the Inner Mongolian suture zone. *Journal of Metamorphic Geology*, 11(4): 511–522.

Wang, C.Z., Jiang, Y., and Xing, G.F., 2011. Recent situation of researches on ophiolites and some problems concerning the ophiolites in south China. *Resources Survey & Environment*, 32(4): 1671–4814.

Wang Dandan, Li Shizhen, Zhou Xingui, Liu Weiwei, Lin Yanhua, Zeng Qiunan and Zhang Wenhao, 2016. SHRIMP U-Pb Dating of Detrital Zircon from the Upper Permian Linxi Formation in Eastern Inner Mongolia，and Its Geological Significance. *Geological Review*, 62(4): 1021–1040 (in Chinese with English abstract).

Wang Jinfang, Li Yingjie, Li Hongyang and Dong Peipei, 2017a. Discovery of Early Permian Intra-oceanic Arc Adakite in the Meilaotewula Ophiolite，Inner Mongolia and its Evolution Model. *Acta Geologica Sinica*, 91(8): 1776–1795 (in Chinese with English abstract).

Wang Jinfang, Li Yingjie and Li Hongyang, 2017b. Zircon LA-ICP-MS U-Pb Age and Island-Arc Origin of the Bayanhua Gabbro in the Hegenshan Suture Zone, Inner Mongolia. *Acta Geologica Sinica* (English Edition), 91(6): 2316–2317.

Wang, Q., and Liu, X.Y., 1986. Paleoplate tectonics between

Cathaysia and Angaral and in Inner Mongolia of China. *Tectonics*, 5(7): 1073–1088.

Wang Shuqing, Hu Xiaojia, Zhao Hualei, Xin Houtian, Yang Zeli, Liu Wengang and He Li, 2017. Geochronology and Geochemistry of Late Carboniferous Jinggesitai Alkaline Granites, Inner Mongolia: Petrogenesis and Implications for Tectonic Evolution. *Acta Geologica Sinica*, 91(7): 1467–1482 (in Chinese with English abstract).

Wang Xiang, 1993. Characteristics of zircon in plagiogranite from Inzecca France and its geological significance. *Chinese Science Bulletin*, 38(6): 534–537 (in Chinese).

Weaver, S.D., Saunder, A.D., Pankhurst, R.J., and Tarney, J., 1979. A geochemical of magmatism associated with the initial stages of back-arc spreading. *Contributions to Mineralogy and Petrology*, 68(2): 151–169.

Whitehead, J., Dunning, G.R., and Spray, J.G., 2000. U-Pb geochronology and origin of granitoid rocks in the Thetford Mines ophiolite, Canadian Appalachians. *Geological Society of America Bulletin*, 112(6): 915–928.

Windley, B.F., Badarch, G., Cunningham, W.D., KrÖner, A., Buchan, A.C., Tomurtogoo, O., and Salnikova, E.B., 2001. Subduction-accretion history of the Central Asian Orogenic Belt: Constraints from Mongolia. *Gondwana Research*, 4(4): 825–826.

Windley, B.F., Alexeiev, D., Xiao, W.J., KrÖner, A., and Badarch, G., 2007. Tectonic models for accretion of the Central Asian Orogenic Belt. *Journal of the Geological Society*, 164(12): 31–47.

Wood, D.A., 1980. The application of Th-Hf-Ta diagram to problems of tectonomagmatic classification and to establishing the nature of crustal contamination of basaltic lavas of the British Tertiary volcanic province. *Earth and Planetary Science Letters*, 50(1): 11–30.

Wu Yuanbao and Zheng Yongfei, 2004. Study on zircon minerageny and its constraints on the interpretation of U-Pb ages. *Chinese Science Bulletin*, 49(16): 1589–1604 (in Chinese).

Xiao, W.J., Windley, B.F., Hao, J., and Zhai, M., 2003. Accretion leading to collision and the Permian Solonker suture, Inner Mongolia, China: Termination of the central Asian orogenic belt. *Tectonics*, 22(6): 1–21.

Xiao, W.J., Windley, B.F., Huang, B.C., Han, C.M., Yuan, C., Chen, H.L., Sun, M., Sun, S., and Li, J.L., 2009. End-Permian to mid-Triassic termination of the accretionary processes of the southern Altaids: Implications for the geodynamic evolution, Phanerozoic continental growth, and metallogeny of Central Asia. *International Journal of Earth Sciences*, 98 (6): 1189–1217.

Xiao, W.J., Huang, B.C., Han, C.M., Sun, S., and Li, J.L., 2010. A review of the western part of the Altaids: A key to understanding the architecture of accretionary orogens. *Gondwana Research*, 18(2–3): 253–273.

Xiao, W.J., Windley, B.F., Allen, M.B., and Han, C.M., 2013. Paleozoic multiple accretionary and collisional tectonics of the Chinese Tianshan orogenic collage. *Gondwana Research*, 23(4): 1316–1341.

Xiao, W.J., and Santosh, M., 2014. The western Central Asian Orogenic Belt: A window to accretionary orogenesis and continental growth. *Gondwana Research*, 25(4): 1429–1444.

Xiao, W.J., Sun, M., and Santosh, M., 2015. Continental reconstruction and metallogeny of the Circum-Junggar areas and termination of the southern Central Asian Orogenic Belt. *Geoscience Frontiers*, 6: 137–140.

Xu, B., and Chen, B., 1997. Framework and evolution of the middle Paleozoic orogenic belt between Siberian and North China Plates in northern Inner Mongolia. *Science in China*, 40 (5): 463–469.

Xu, B., Charvet, J., Chen, Y., Zhao, P., and Shi, G.Z., 2013. Middle Paleozoic convergent orogenic belts in western Inner Mongolia (China): framework, kinematics geochronology and implications for tectonic evolution of the Central Asian Orogenic Belt. *Gondwana Research*, 23(4): 1342–1364.

Yang , J., Zhang, Z., Chen, Y., Yu, H., and Qian, X., 2017. Ages and origin of felsic rocks from the Eastern Erenhot ophiolitic complex, southeastern Central Asian Orogenic Belt, Inner Mongolia China. *Journal of Asian Earth Sciences*, 144: 126–140.

Yin Zhengxin,Yuan Yajuan, Lü Baofeng, Cai Zhourong, Zheng Hao, Huang Qiangtai, Xia Bin, Zhong Yun, Xia Zhongyu, Shi Xiaolong and Guan Yao, 2015. Zircon U-Pb geochronology and Hf isotopic constraints on petrogenesis of plagiogranite from the Cuomuqu ophiolite, Bangong lake area, north Tibet. *Acta Geologica Sinica* (English Edition), 89(2):418–440.

Yoshikawa, M., and Ozawa, K., 2007. Rb-Sr and Sm-Nd isotopic systematics of the Hayachine-Miyamori ophiolitic complex: melt generation process in the mantle wedge beneath an Ordovician island arc. *Gondwana Research*, 11(1–2): 234–246.

Yuan, H.L., Gao, S., Liu, X.M., Li, H.M., Günther, D., and Wu, F.Y., 2004. Accurate U-Pb age and trace element determinations of zircon by laser ablation-inductively coupled plasma-mass spectrometry. *Geostandards and Geoanalytical Research*, 28(3): 353–370.

Zeng, L., Niu, H., Bao, Z., Shan, Q., Li, H., Li, N.B., and Yang, W.B., 2015. Petrogenesis and tectonic significance of the plagiogranites in the Zhaheba ophiolite, Eastern Junggar orogen, Xinjiang, China. *Journal of Asian Earth Sciences*, 113: 137–150.

Zhang Qi, Wang Yan, Xiong Xiaolin, Li Chengdong., 2008. *Adakite and Granite: Challenge and Opportunity*. Beijing: China Land Press, 29–30 (in Chinese with English abstract).

Zhang, Z.C., Li, K., Li, J.F., Tangy, W.H., Chen, Y., and Luo, Z.W., 2015a. Geochronology and geochemistry of the eastern Erenhot ophiolitic complex: Implications for the tectonic evolution of the Inner Mongolia-Daxinganling Orogenic Belt. *Journal of Asian Earth Sciences*, 97(Part B): 279–293.

Zhang, Z.C., Li, K., Li, J.F., Tang, W.H., Chen, Y., and Luo, Z.W., 2015b. Geochronology and geochemistry of the eastern Erenhot ophiolitic complex: Implications for the tectonic evolution of the Inner Mongolia-Daxinganling Orogenic Belt. *Journal of Asian Earth Sciences*, 97(Part B): 279–293.

Zhang, X.H., Wilde, S.A., Zhang, H.F., and Zhai, M.G., 2011. Early Permian high-K calc-alkaline volcanic rocks from NW Inner Mongolia, North China: geochemistry, origin and tectonic implications. *Journal of the Geological Society*, 168 (2): 525–543.

Zhang Yongsheng, Peng Yuan, Shi Lizhi, Xing Enyuan, Gui Baolin and Li Kai, 2017. Molecular Biomarker Characteristics of the Linxi Formation Source Rocks in the Middle-Western Region of Inner Mongolia: New evidence for late-stage tectonic evolution of the Paleo-Asian Ocean. *Acta Geologica Sinica* (English Edition), 91(2): 745–746.

Zhao, P., Chen, Y., Xu, B., Faure, M., Shi, G.Z., and Choulet, F., 2013. Did the Paleo-Asian Ocean between North China Block and Mongolia Block exist during the late Paleozoic? First paleomagnetic evidence from central-eastern Inner Mongolia, China. J*ournal of Geophysical Research-solid Earth,* 118: 1873–1894. http://dx.doi.org/10.1002/jgrb.50198.

Zhao, P., Xu, B., Tong, Q.L., Chen, Y., and Faure, M., 2016. Sedimentological and geochronological constraints on the Carboniferous evolution of central Inner Mongolia, southeastern Central Asian Orogenic Belt: Inland sea deposition in a post-orogenic setting. *Gondwana Research*, 31: 253–270.

Zhu Junbing and He Zhengjun, 2017. Detrital Zircon Records of Upper Permian Middle Triassic Sedimentary Sequence in the Linxi Area, Inner Mongolia and Constraints on Timing of Final Closure of the Paleo-Asian Ocean (Eastern Segment). *Acta Geologica Sinica*, 91(1): 232–248 (in Chinese with English abstract).

Zhu Junbin and Ren Jishun, 2017. Carboniferous-Permian Stratigraphy and Sedimentary Environment of Southeastern Inner Mongolia, China: Constraints on Final Closure of the Paleo-Asian Ocean. *Acta Geologica Sinica* (English Edition), 91(3): 832–856.

About the first author

LI Yingjie, female, born in 1976 in Jining City, Shandong Province; doctor; graduated from China University of Geosciences, Beijing; associate professor of School of Nature Resources, Hebei GEO University. She is now interested in the study on igneous rocks and tectonic environments. Email: yingjieli820@163.com; phone: 0311-87207655, 15632364069.